

72789

DOKUZ EYLÜL UNIVERSITY
INSTITUTE OF SCIENCE AND TECHNOLOGY

INVESTIGATION OF STRESS DISTRIBUTION
IN THE TRANSVERSE FILLET WELD JOINT

M.S. Degree Thesis

By
Muhammed CERİD

Y. G.
Yükseköğretim Kurulu
Dokümantasyon Merkezi
Supervisor
Doç.Dr. Onur SAYMAN

August, 1990
Bornova-İZMİR

INVESTIGATION OF STRESS DISTRIBUTION IN THE TRANSVERSE FILLET WELD JOINT

CERİD, Muhammed

M.S. in Mech. Eng.

Supervisor: Doç.Dr.Onur SAYMAN

August. 1990 69 pages

ABSTRACT

In the transverse fillet weld joint under the tensile force, the stress distributions of the weld metal and the welded plates are investigated by the finite element method. Weld metal material and material of the welded plates are accepted as the same. In the analysis, three and six-node plane triangular finite elements are used. We have written the programme in the APL programming language for the mesh generation of the domain of the problem and for calculation of the stresses.

In each direction under consideration of weld metal and welded plates, the stress distributions are plotted in dimensionless coordinates, stresses versus lengths, for individual components of the calculated plane stresses σ_x , σ_y and τ_{xy} and also, principle stresses σ_1 and σ_2 , and maximum shear stress τ_{max} . The distribution from the analysis for the weld metal are compared with the experimental one, by photoelastic method, in literature. It is observed that the obtained characteristic of the stress distribution for the weld metal is convenient with the one by photoelastic way. The analysis are also extended to the welded plates, lap and center plates.

Stress distributions of the different lengths of lap plate, are investigated, in addition to other distributions, for driving the some conclusions to make the best one of transverse fillet weld joints from point of view of the stress analysis.

Key words: Welding, fillet welds, transverse fillet welds, joints, lap joints, stress distributions.

BİNDİRME KAYNAK BAĞLANTISINDA GERİLME DAĞILIMININ İNCELENMESİ

CERİD, Muhammed
Y.Lisans Tezi, Makina Müh. Bölümü
Tez Yöneticisi: Doç.Dr.Onur SAYMAN
Ağustos 1990, 69 sayfa

ÖZ

Eksenel çekme kuvveti etkisinde, bindirme (köşe) kaynağında, kaynak metalinde ve kaynaklanan levhalarda meydana gelen gerilme dağılımları sonlu eleman metodu ile incelendi. İncelemede, kaynak metali ve kaynaklanan levhalar aynı malzemeden kabul edildi. Gerilme analizi yapılırken üç ve altı düğümlü düzlem üçgen sonlu elemanlar kullanıldı. Problem bölgesinin elemanlara bölünmesi ve gerilmelerin hesaplanması, bilgisayarda, APL dilinde yazılan bir programla gerçekleştirildi.

Kaynak metalinde ve kaynaklanan levhalarda çeşitli doğrultular üzerinde, düzlem gerilme bileşenleri σ_x , σ_y ve τ_{xy} ve bunlara bağlı hesaplanan asal gerilme bileşenleri σ_1 , σ_2 ve maksimum kayma gerilmesi τ_{max} değişimleri boyutsuz, uzunluk-gerilme eksenlerinde grafikler halinde gösterildi. Kaynak metalinde meydana gelen gerilme dağılımları, literatürde deneysel (fotoelastik) metotla elde edilen gerilme dağılımları ile karşılaştırıldı. Buna ek olarak levhalardaki (merkez levha ve bindirme levha) gerilme dağılımları da incelendi.

Kaynaklanan levhalardan, bindirme levhasının farklı boyları için gerilme dağılımı araştırıldı. Bulunan sonuçlardan gerilme analizi açısından, bindirme kaynağı ile yapılan birleştirmede en uygun bağlantının boyutsal özellikleri konusunda bazı sonuçlar çıkarılmaya çalışıldı.

Anahtar sözcükler: Kaynak, köşe/(bindirme) kaynağı, kaynak bağlantıları, gerilme dağılımları.

NOMENCLATURE

The symbols are listed roughly in order of occurrence in the text

F	Force
h	Height of the plates, length of weld legs
l	Length of the weld
A	Cross section of the weld or plate
σ_x	Normal stress in the x-direction
σ_y	Normal stress in the y-direction
σ_1	Maximum principal stress
σ_2	Minimum principal stress
τ_{xy}	Shear stress
τ_{max}	Maximum shear stress
δ	Displacement vector
δ_u	Element displacements vector of x-direction
δ_v	Element displacements vector of y-direction
ξ	Vector of strains ϵ_x , ϵ_y and γ_{xy}
ξ_e	Vector of primary strains due to mechanical forces
ξ_0	Vector of secondary strains due to thermal and residual effects
σ	Stress vector, or normal stress
D	Matrix of elasticity
Π	Strain energy density
B	Strain-displacement transformation matrix of the element
Q	Total potential energy
P_e	Mechanical load vector
P_0	Initial force vector
K	Stiffness matrix
P_t	Total load vector
J	Jakobian operator
x	Coordinate in x-direction
X	Vector of x-coordinates of the nodes of the element
y	Coordinate in y-direction
Y	Vector of y-coordinates of the nodes of the element
N_i	Shape function of the node i
u	Nodal displacement in the x-direction
v	Nodal displacement in the y-direction
i	Number of element

IV

n	Node number of element
T	Transpose of matrix
H, S	Natural coordinates
N	Shape functions vector
ψ	Vector of variables of isoparametric natural coordinates
Ω	Square matrix consists of constants
ϵ_x	Component of the strain in the x-direction
ϵ_y	Component of the strain in the y-direction
γ_{xy}	Shearing strain
B_i	Strain-displacement transformation matrix of the node i
δ_i	Displacements of node i
R	Thermal and residual effect energy term
E	Elasticity modulus
ν	Poisson's ratio
η	Non-dimensional stress coordinate axis equal to σ / σ_0 or σ / σ_0^I
χ	Non-dimensional length coordinate axis equal to l/h
σ	$\sigma_x, \sigma_y, \tau_{xy}, \sigma_1, \sigma_2$ and τ_{max}
l	Lengths l, L_1, L_2 etc.
σ_0	Nominal stress, F/hl
σ_0^I	Nominal stress, $2F/hl$

CONTENTS

	<u>Page</u>
ABSTRACT	I
ÖZ	II
NOMENCLATURE	III
LIST OF THE FIGURES AND TABLES.....	VII
ACKNOWLEDGEMENTS.....	IX
CHAPTER I	1
1. INTRODUCTION	1
1.1. The Defination Of The Problem Studied	2
1.2. Stress Distribution İn Fillet Welds İn Literature..	4
1.3. On Determination Of Stress Distribution İn Fillet Weld	8
CHAPTER II	
2. FINITE ELEMENT PROCEDURE	9
2.1. The Stiffness Derivative Development	9
2.2. The Stiffness Matrix Derivation Of The Triangle Element	13
CHAPTER III	
3. CONSTRUCTING THEORETICAL MODEL	23
3.1. Finite Element Model Of The Problem For Stress Analysis	23
3.1.1. Boundary Conditions	25
3.1.2. Mesh Generation	25
3.2. Displacement-Strain Relations In Plane	27
3.3. Stress-Strain Relationships	27
3.4. Material Properties	28
3.5. The Numerical Values Used In The Study	28

	<u>Page</u>
CHAPTER IV	
4. RESULTS AND DISCUSSION	29
4.1. The Stress Distribution In Weld Metal	29
4.1.1. The Stress Distribution On The Weld Leg BC	29
4.1.2. The Stress Distribution On The Weld Leg AB	32
4.1.3. The Stresses Across The Throat DB Of The Weld	36
4.2. The Distributions Of The Stresses In The Welded Plates	39
4.2.1. The Stresses In The Center Plate	39
4.2.2. The Stresses In The Lap Plate	42
CHAPTER V	
CONCLUSIONS	46
REFERENCES	48
APPENDIX	
THE COMPUTER PROGRAMME	50
LIST OF THE COMPUTER PROGRAMME	51

LIST OF THE FIGURES AND TABLES

	<u>Page</u>
Figure 1.1. Arc weld symbols	2
Figure 1.2. Some of the fillet weld joints	2
Figure 1.3. A transverse fillet weld lap joint investigated	3
Figure 1.4. A transverse fillet weld	6
Figure 1.5. A portion of the weld has been selected for free body	6
Figure 1.6. Plane element is selected on DB	6
Figure 1.7. Morh's Circle	6
Figure 1.8. Stress distribution in fillet welds	7
Figure 2.1. Coordinate systems and nodal points	14
Figure 2.2. Interpolation functions of three to six variable number nodes two dimensional trianle	14
Figure 3.1. The general arrangement of the transverse fillet weld joint investigated	23
Figure 3.2. A quarter of the joint which is shaded analysed	23
Figure 3.3. Different directions of the model on which stresses distributions investigated	24
Figure 3.4. The finite element model of the symmetric quarter of the joint investigated.....	26
Figure 4.1. Normal stress distribution on the leg BC ..	30
Figure 4.2. Normal stress distribution on the leg BC ..	30
Figure 4.3. Distributions of the principal stresses and max. shear stress on the leg BC	31
Figure 4.4. Normal stress distribution on the leg AB ..	33
Figure 4.5. Distributions of normal stress and shear stress on the leg AB	34
Figure 4.6. Distributions of principal stresses and maximum shear stress on the leg AB	35
Figure 4.7. Normal stress distribution on the troath DB of the weld	37
Figure 4.8. Distributions of normal stress and shear stress on the troath DB of the weld	37
Figure 4.9. Distributions of the principal stresses and maximum shear stress on the troath DB of weld	38

VIII

	<u>Page</u>
Figure 4.10. Normal stress distribution on the EF in the center plate	40
Figure 4.11. Distributions of normal stress and shear stress on the EF in the center plate	40
Figure 4.12. Distributions of the principal stresses and maximum shear stress on the EF in the center plate	41
Figure 4.13. Stresses distributions of MN in the lap plate	43
Figure 4.14. The variation of the σ_x in different thicknesses along the length of the lap plate	44
Table 4.1. Some of the stresses values on the JH in the center plate	45
Table 1. All of the values of the stresses from computer	59



ACKNOWLEDGEMENTS

I am deeply grateful to Doç.Dr. Onur Sayman for his patient supervision, valuable guidance and continuous encouragement throughout this study.

I am much indebted to Yrd.Doç.Dr. Durmuş Günay, Istanbul Technical University, Sakarya Engineering Faculty, Adapazarı, for his active support and his continued interest in my work.

I also would like to extend very thanks to Doç.Dr. Mehmet Tekeliođlu and Research Ass. Ramazan Karakuzu, for their supports and helpful suggestions in preparing computer programme, in the computer center, Engineering-Architecture Faculty, Dokuz Eylül University, Bornova.

Very thanks to İlyas Korkmaz, who is in printing office of Sakarya Engineering Faculty, for his outstanding job in typing the manuscript.

Sincere thanks are also due to my friend Ođuzhan Özer for his helps in drawing the graphs.

Muhammed Cerid

Adapazarı, Turkey

CHAPTER I

1. INTRODUCTION

Process welding is used extensively in manufacturing today. Whenever parts have to be assembled or fabricated, there is usually good cause for considering the welding as one of joint processes in preliminary design work. Especially, when the sections to be joined are thin, welding may lead to significant savings.

A weldment is fabricated by welding together a collection of metal shapes, cut to particular configurations.

One of the most important problems in welded joints is the calculations of the stresses in the welds. Sometimes, the methods of strength of materials in practice are not sufficient in determination of stress distribution of weld joints in acceptable approximation. Attempts to solve for the stress distribution in such welds, using methods of elasticity, also, have not been very successful. In such cases, we may apply the one of the numerical analysis methods, such as the finite element method.

The finite element, which is very powerful and elegant numerical analysis method, is used widely in stress analysis today.

Thus, in present study, we have investigated the stress distributions in transverse fillet weld joint, in weld metal and in parent (welded) metal by using the finite element method.

1.1. THE DEFINATION OF THE PROBLEM STUDIED

In the study, it is studied stress distributions in a weld joint, which is called "transverse fillet weld joint", as shown in figure (1.3). It is note that there are several fillet welds specified, by American Welding Society (AWS) with respect to type of the weld (see figure 1.1),









Type of weld							
Beod	Fillet	plug or slot	Groove				
			Square	V	Bevel	U	J
							

Figure:1.1. Arc weld symbols

and/or position of parent plates (see figure 1. b, c and d) or loading conditions (see figure 1.2. a, c)

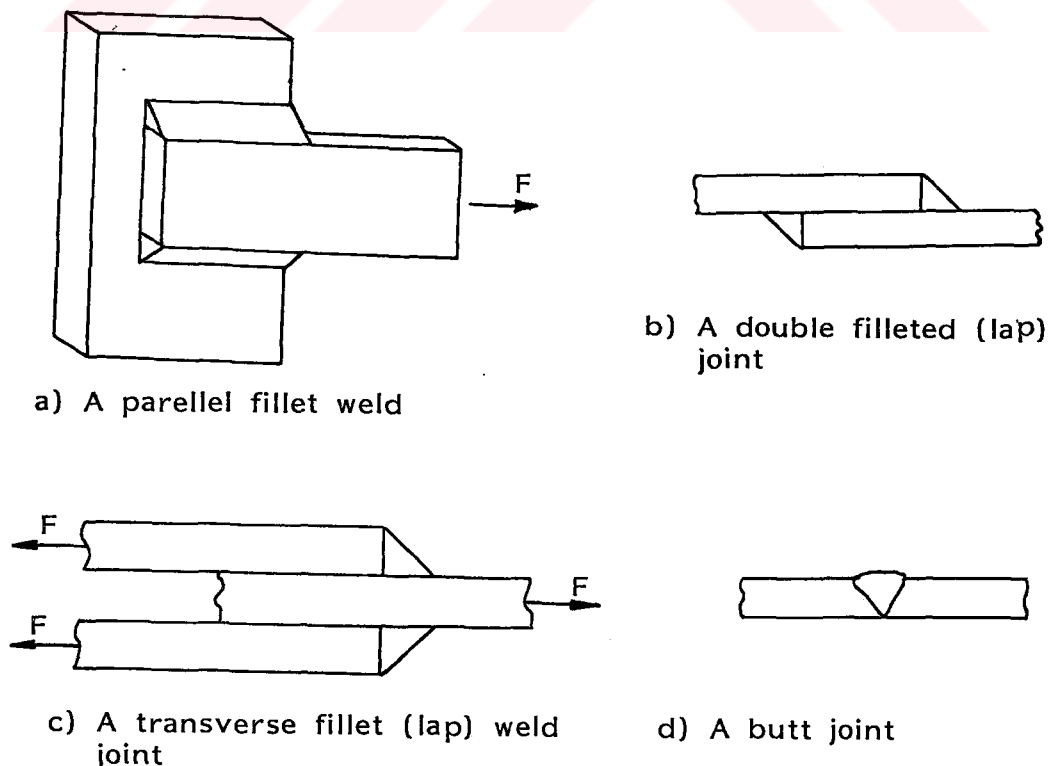


Figure: 1.2. Some of the fillet weld joints

In figure (1.2a), the force is parallel to the weld direction and, the type of weld is fillet, that is why it is titled as "a parallel fillet weld".

In figure (1.2b), the joint has two fillets and plates are lapped one another so it is called "double filleted (lap) joint".

Under the above explanations, the problem we have engaged can be specified as the title "Transverse Fillet Weld Lap Joint".

But in practice, common usage for the weld joint is "Transverse Fillet Weld Joint" so we will also use the same title in the next chapters.

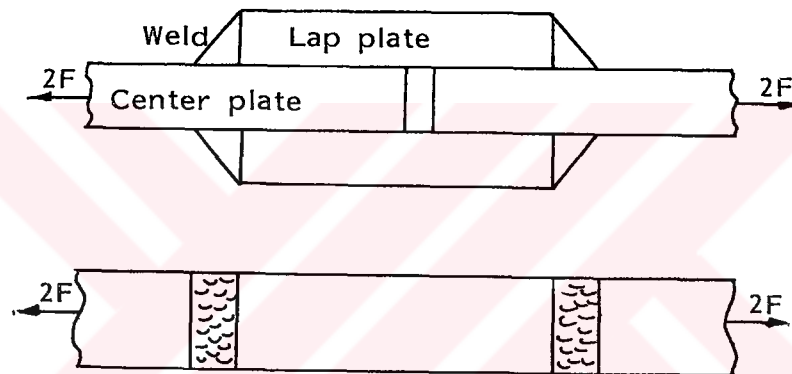


Figure: 1.3. A transverse fillet weld lap joint investigated

1.2. STRESS DISTRIBUTION IN FILLET WELDS IN LITERATURE

A typical transverse fillet weld is shown in figure(1.4). Attempts to solve for the stress distribution in such welds, using the methods of theory of elasticity, have not been very successful. Conventional practice in welding engineering design has always been to base the size of the weld upon the magnitude of the stress on the throat area DB.

In figure(1.5) a portion of the weld has been selected from figure(1.4) so as to treat the weld throat as a problem in free-body analysis. The throat area is

$$A = h l \cos 45^\circ = 0.707 h l$$

Where l is the length of the weld. Thus the stress σ_x is

$$\sigma_x = \frac{F}{A} = \frac{F}{0.707 h l} \quad (1.1)$$

This stress can be divided into two components, a shear stress τ and a normal stress σ . These are

$$\tau = \sigma_x \cos 45^\circ = \frac{F}{h l} \quad (1.2)$$

$$\sigma = \sigma_x \cos 45^\circ = \frac{F}{h l} \quad (1.3)$$

In figure(1.7) these are entered into a Mohr's circle diagram. The largest principal stress is seen to be

$$\sigma_1 = \frac{F}{2hl} + \sqrt{\left(\frac{F}{2hl}\right)^2 + \left(\frac{F}{hl}\right)^2} = 1.618 \frac{F}{hl} \quad (1.4)$$

also the minimum principal stress is

$$\sigma_2 = \frac{F}{2hl} - \sqrt{\left(\frac{F}{2hl}\right)^2 + \left(\frac{F}{hl}\right)^2} = -0.618 \frac{F}{hl} \quad (1.5)$$

and the maximum shear stress is

$$\tau_{\max} = \sqrt{\left(\frac{F}{2hl}\right)^2 + \left(\frac{F}{hl}\right)^2} = 1.118 \frac{F}{hl} \quad (1.6)$$

However, for design purposes it is customary to base the shear stress on the throat area and to neglect the normal stress altogether. Thus the equation for average stress is,

$$\tau = \frac{F}{0.707hl} = 1.414 \frac{F}{hl} \quad (1.7)$$

and is normally used in designing joints having fillet welds. Note that, this gives a shear stress

$$\frac{1.414}{1.118} = 1.26 \text{ times greater than that given by equation (1.6)}$$

There are some experimental and analytical results that are helpful in evaluating equation (1.7). A model of the transverse fillet weld of figure (1.4) is easily constructed for photoelastic purposes and has the advantage of a balanced loading condition. Norris constructed such a model and reported the stress distribution along the sides AB and BC of the weld. *An approximate graph of the results he obtained is shown as figure (1.8a). Note that stress concentration exists at A and B on the horizontal leg and at B on the vertical leg. Norris states that he could not determine the stresses at A and B with any certainty.

* C.H. Norris, "Photoelastic Investigation of Stress Distribution in Transverse Fillet Welds", *Welding J.*, vol. 24, 1945, p.557s.

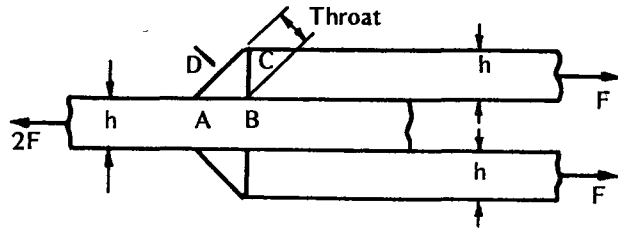


Figure: 1.4 A transverse fillet weld

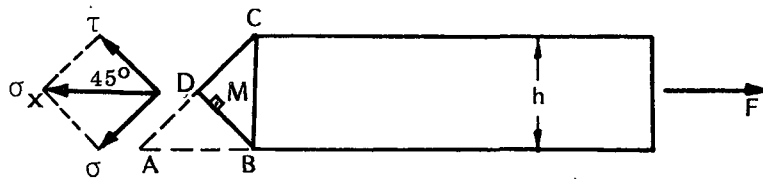


Figure: 1.5. A portion of the weld has been selected for free body

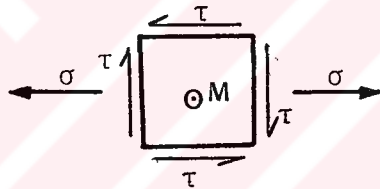


Figure: 1.6. Plane element is selected on DB

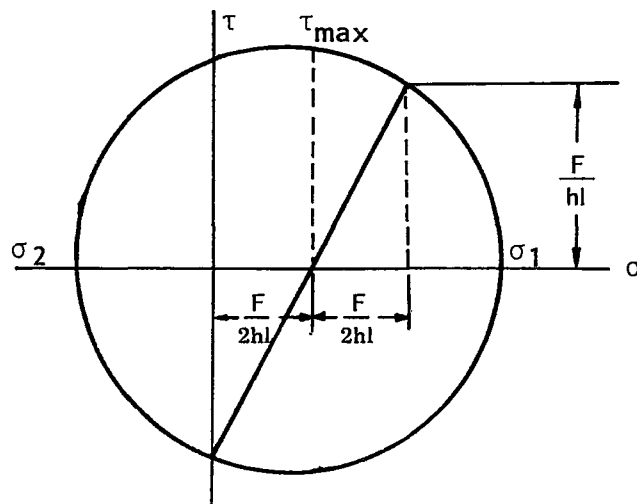


Figure: 1.7. Morh's Circle

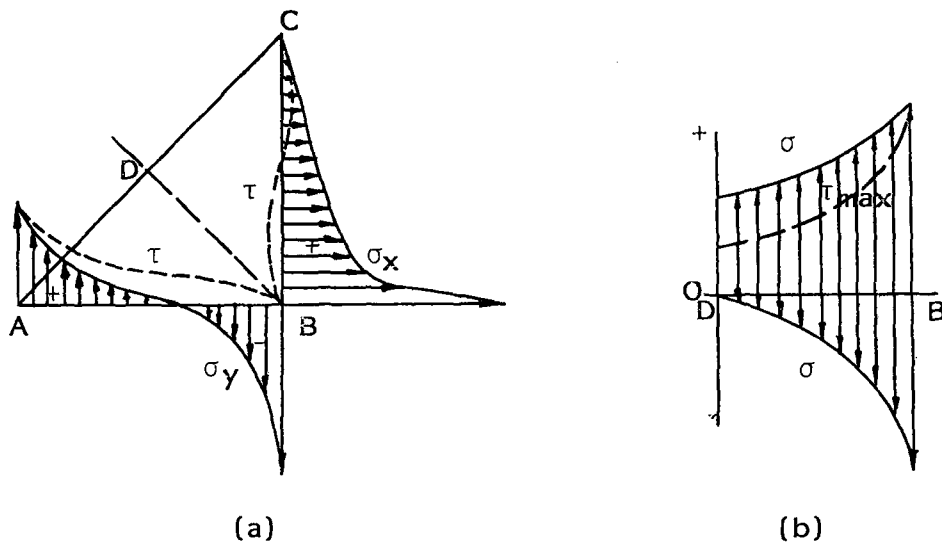


Figure: 1.8. Stress distribution in fillet welds. a) Stress distribution on the legs as reported by Norris.. b) Distribution of principal stresses and maximum shear stress as reported by salakian

Salakian† presents data for the stress distribution across the throat of a fillet weld figure(1.8b). This graph is of particular interest because we have just learned that it is the throat stresses that are used in design. Again, the figure shows stress concentration at point B. Note that figure(1.8a)applies either to the weld metal or to the parent metal and that figure (1.8b)applies only to the weld metal.

†A.G. Salakian and G.E.Claussen, "Stress Distribution in Fillet Welds; A Review of the Literature", Welding J., vol. 16, May 1937, pp. 1-24.

1.3. ON DETERMINATION OF STRESS DISTRIBUTION IN FILLET WELD

As seen from the summary of studies about stress distribution in fillet welds in literature, all of them experimental. It is given variation of the stress qualitatively. But there is no calculation of accurate values of the stresses in the critical points in the weld (A, B, C, D). The graphs given in figure (1.8) are obtained photoelastic method. They belong to weld metal. | 7 | and | 10 |

In this investigation, we have calculated the stress in parent metal (welded plates) by finite element method, as well as weld metal. From the values of stresses calculated, we have plotted variation of stresses in the transverse fillet weld, legs of weld as well as in horizontal and vertical directions of the lap and center plates welded. From the characteristic of the variation stresses in different directions of weld metal and parent metal, and from magnitudes of stresses at the critical points, we have tried to derive some conclusions about the welding of transverse fillet weld joint.

In the study, we have used the finite element method. Thus, we have showed the general procedure which how the method work, and we have derived the formulation of the triangular finite element used in the study. In the formulation, element stiffness matrix K is derived by using minimum potential energy principle.

It is also emphasized that how we will achieve the transformation from the physical case of the problem into the theoretical model.

CHAPTER II

2. FINITE ELEMENT PROCEDURE

2.1. THE STIFFNESS DERIVATIVE DEVELOPMENT

Development of the elasticity equations for the finite element solutions involves the use of matrix notation for the variables, as the equations are representative of systems with many degrees of freedom. For example, the finite element solution of this work employ the two-dimensional, six node triangular element. The element has two degrees of freedom at each node and its nodal displacement vector is expressed as

$$\delta = (u_1, v_1, u_2, v_2, \dots, u_6, v_6)^T \quad (2.1)$$

Note that, this is the vector for an individual element, and T specifies the transpose of the designated matrix. The total strain vector at a point on the element is

$$\xi = \xi_e + \xi_o \quad (2.2)$$

in which ξ_e represents the primary strains which result from mechanical forces, and ξ_o represents the secondary strains which are due to thermal or residual effects.

The stress vector at this point is

$$\sigma = D \xi_e = D (\xi - \xi_o) \quad (2.3)$$

in this equation, D is a proportionately matrix consisting of elastic constant of Young's modulus E and Poisson's ratio ν . It is a square symmetric matrix, and therefore

$$D^T = D \quad (2.4)$$

The total strain vector and nodal displacement vector are related by means of the B matrix, the terms of which are derivatives of the

element shape function at the specified point

$$\xi = B \delta \quad (2.5)$$

The expression for the strain energy density at the point of interest is

$$\Pi = \frac{1}{2} \sigma^T \xi_e = \frac{1}{2} \sigma^T (\xi - \xi_0) \quad (2.6)$$

From equations (2.3) and (2.4)

$$\sigma^T = (\xi^T - \xi_0^T) D^T = (\xi^T - \xi_0^T) D \quad (2.7)$$

From equation (2.5)

$$\xi^T = \delta^T B^T \quad (2.8)$$

Substituting the previous two equations into equation (2.6) results in

$$\Pi = \frac{1}{2} (\delta^T B^T - \xi_0^T) D (B \delta - \xi_0) \quad (2.9)$$

which expands to

$$\Pi = \frac{1}{2} \delta^T B^T D B \delta - \frac{1}{2} \delta^T B^T D \xi_0 - \frac{1}{2} \xi_0^T D B \delta^T + \frac{1}{2} \xi_0^T D \xi_0 \quad (2.10)$$

the third term of this expression is equal to its transpose, and can therefore be combined with the second term to produce

$$\Pi = \frac{1}{2} \delta^T B^T D B \delta - \delta^T B^T D \xi_0 + \frac{1}{2} \xi_0^T D \xi_0 \quad (2.11)$$

The strain energy of the element Π is calculated by integrating the strain energy density of the element volume V

$$\begin{aligned} \Pi = \int \Pi \, dV = & \frac{1}{2} \delta^T \left(\int B^T D B^T \, dV \right) \delta - \delta^T \int B^T D \xi_0 \, dV + \\ & + \frac{1}{2} \int \xi_0^T D \xi_0 \, dV \end{aligned} \quad (2.12)$$

The total potential energy of the element is defined as

$$Q = \Pi - \delta^T P_e \quad (2.13)$$

where P_e is the mechanical load vector which causes the primary strains, in addition

$$P_o = \int B^T D \xi_o dV \quad (2.14)$$

where P_o is the load vector related to the secondary strains in the element. The element stiffness matrix is defined as

$$K = \int B^T D B dV \quad (2.15)$$

and

$$R = \frac{1}{2} \int \xi_o^T D \xi_o dV \quad (2.16)$$

Using equations (2.14) through (2.16), the total potential energy can be written as

$$Q = \frac{1}{2} \delta^T K \delta - \delta^T P_o + R + \delta^T P_e \quad (2.17)$$

This expression is defined for element and the overall structural application.

The total load vector can be written as

$$P_t = P_e + P_o \quad (2.18)$$

In the overall sense, the load vector P_e corresponds to loads that are applied externally since the internal forces all cancel at the internal nodes due to equilibrium considerations (2.6). The total potential energy for the overall structure is

$$Q = \frac{1}{2} \delta^T K \delta - \delta^T P_t + R \quad (2.19)$$

In the current study, the thermal and residual effects are negligible and, therefore,

$$P_o = R = 0 \quad (2.20)$$

and

$$Q = \frac{1}{2} \delta^T K \delta - \delta^T P_e \quad (2.21)$$

Applying minimum potential energy principle, which is,

$$\frac{\partial Q}{\partial \delta} = 0 \quad (2.22)$$

from equation (2.21)

$$\frac{\partial Q}{\partial \delta} = \frac{\partial}{\partial \delta} \left(\frac{1}{2} \delta^T K \delta \right) - \delta^T P_e = 0$$

and we have

$$K \delta = P_e \quad (2.23)$$

$$K = \int B^T D B \, dV \quad (2.24)$$

where

$$dV = t \, |J| \, dH \, dS$$

2.2. THE STIFFNESS MATRIX DERIVATION OF THE TRIANGLE ELEMENT

When used in the solution of plane problems every member of triangle elements, of three nodes or six nodes, has two (displacement) degrees of freedom per node. The cartesian coordinates, used general coordinate system, at any point on an element are expressed in terms of node coordinates of the element by using shape functions as,

$$x = \sum_{i=1}^n N_i x_i$$

$$y = \sum_{i=1}^n N_i y_i$$
(2.25)

in which N_i is shape function of the node i ; x_i and y_i are cartesian coordinates of the node i ; and n denotes the node number of the element.

The displacements (u, v) at any point on the an element are expressed, in a similar way of equation (2.25) in terms of nodal displacements by using shape functions as,

$$u = \sum_{i=1}^n N_i u_i$$

$$v = \sum_{i=1}^n N_i v_i$$
(2.26)

in which u_i and v_i are displacements of the node i .

The general coordinate system (cartesian coordinates x and y) and the isoparametric natural coordinate system (coordinates H and S) are illustrated in figure(2.1).

The shape functions are given |1| in the figure(2.2).

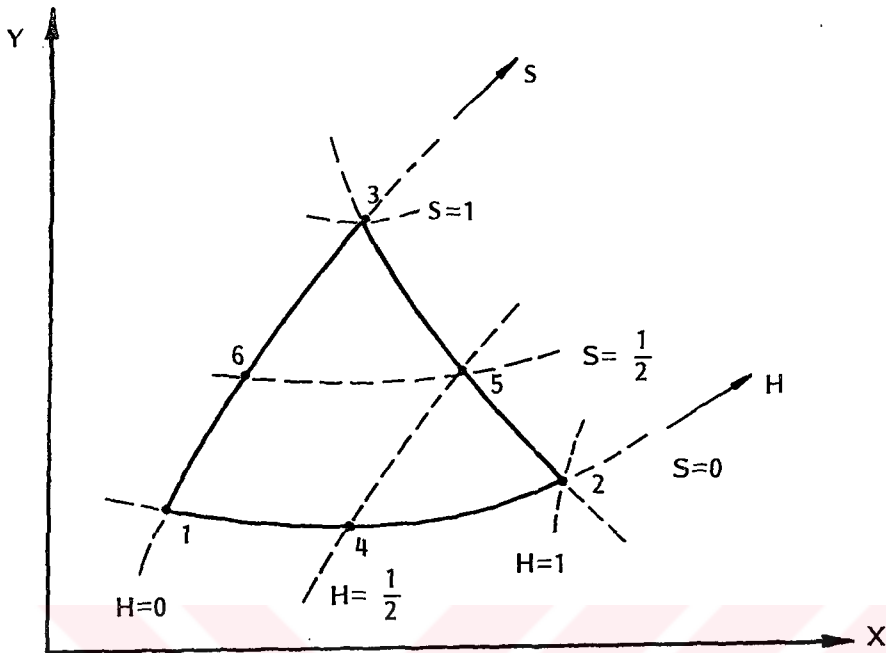


Figure:2.1 Coordinate systems and nodal points

Include only if node i is define

		i=4	i=5	i=6
$N_1 =$	1-H-S	$-\frac{1}{2} N_4$	$-\frac{1}{2} N_6$
$N_2 =$	H	$-\frac{1}{2} N_4$	$-\frac{1}{2} N_5$
$N_3 =$	S	$-\frac{1}{2} N_5$	$-\frac{1}{2} N_6$
$N_4 =$	$4H(1-H-S)$			
$N_5 =$	$4HS$			
$N_6 =$	$4S(1-H-S)$			

Figure: 2.2 Interpolation functions of three to six variable number nodes two dimensional triangle

H and S are isoparametric natural coordinates, and H_i and S_i denote the isoparametric natural coordinates of the node i.

For the six-node triangle element, the shape functions are presented explicitly in the below.

$$\begin{aligned}
 N_1 &= 1 - 3H - 3S + 2H^2 + 4HS + 2S^2 \\
 N_2 &= -H + 2H^2 \\
 N_3 &= -S + 2S^2 \\
 N_4 &= 4H - 4H^2 - 4HS \\
 N_5 &= 4HS \\
 N_6 &= 4S - 4HS - 4S^2
 \end{aligned}
 \tag{2.27}$$

The shape functions can be define as,

$$N = \psi \Omega \tag{2.28}$$

in equation (2.28), N is the shape functions vector consists of the node shape functions,

$$N = [N_1, N_2, \dots, N_6] \tag{2.29}$$

ψ is of order n, the number of nodes in the element, and consists of variables of isoparametric natural coordinates. For six node-triangle,

$$\psi = [1, H, S, H^2, HS, S^2] \tag{2.30}$$

and for three-node triangle,

$$\psi = [1, H, S] \tag{2.31}$$

The square matrix Ω is also of order n, and consists of constants. For six node-triangle

$$\Omega = \begin{bmatrix} 1 & 0 & 0 & 0 & 0 & 0 \\ -3 & -1 & 0 & 4 & 0 & 0 \\ -3 & 0 & -1 & 0 & 0 & 4 \\ 2 & 2 & 2 & -4 & 0 & 0 \\ 4 & 0 & 0 & -4 & 4 & -4 \\ 2 & 0 & 2 & 0 & 1 & -4 \end{bmatrix} \quad (2.32)$$

and for three node-triangle

$$\Omega = \begin{bmatrix} 1 & 0 & 0 \\ -1 & 1 & 0 \\ 1 & 0 & 1 \end{bmatrix} \quad (2.33)$$

The coordinates of any point on the elements, given in equation (2.25) can also be expressed by using the shape functions vector as,

$$\begin{aligned} x &= N X \\ y &= N Y \end{aligned} \quad (2.34)$$

in which N is shape functions vector given in equation (2.28), X and Y are vectors in terms of x and y coordinates of the nodes of the element, respectively.

$$\begin{aligned} X^T &= [x_1, x_2, \dots, x_6] \\ Y^T &= [y_1, y_2, \dots, y_6] \end{aligned} \quad (2.35)$$

In similar manner

$$\begin{aligned} u &= N \delta u \\ v &= N \delta v \end{aligned} \quad (2.36)$$

In which u and v are displacements at any point on the triangle in direction x and y respectively. And δu and δv are nodal displacements vector in direction x and y respectively.

$$\begin{aligned} \delta u^T &= [u_1, u_2, \dots, u_6] \\ \delta v^T &= [v_1, v_2, \dots, v_6] \end{aligned} \quad (2.37)$$

The strain-displacement relation for plane is given as

$$\xi = \begin{Bmatrix} \epsilon_x \\ \epsilon_y \\ \gamma_{xy} \end{Bmatrix} = \begin{Bmatrix} \frac{\partial u}{\partial x} \\ \frac{\partial v}{\partial y} \\ \frac{\partial u}{\partial y} + \frac{\partial v}{\partial x} \end{Bmatrix} \quad (2.38)$$

Derivatives of displacements with respect to cartesian coordinates expand to,

$$\begin{aligned} \frac{\partial u}{\partial x} &= \frac{\partial (N \delta u)}{\partial x} \\ &= \frac{\partial N_1}{\partial x} u_1 + \frac{\partial N_2}{\partial x} u_2 + \dots + \frac{\partial N_6}{\partial x} u_6 \end{aligned}$$

$$\begin{aligned} \frac{\partial v}{\partial y} &= \frac{\partial (N \delta v)}{\partial y} \\ &= \frac{\partial N_1}{\partial y} v_1 + \frac{\partial N_2}{\partial y} v_2 + \dots + \frac{\partial N_6}{\partial y} v_6 \end{aligned}$$

and

$$\begin{aligned} \frac{\partial u}{\partial y} + \frac{\partial v}{\partial x} &= \frac{\partial (N \delta u)}{\partial y} + \frac{\partial (N \delta v)}{\partial x} \\ &= \frac{\partial N_1}{\partial y} u_1 + \frac{\partial N_2}{\partial y} u_2 + \dots + \frac{\partial N_6}{\partial y} u_6 \\ &\quad + \frac{\partial N_1}{\partial x} v_1 + \frac{\partial N_2}{\partial x} v_2 + \dots + \frac{\partial N_6}{\partial x} v_6 \end{aligned}$$

The strain vectors, therefore can be written as,

$$\xi = \left\{ \begin{array}{l} \frac{\partial N_1}{\partial x} u_1 + \frac{\partial N_2}{\partial x} u_2 + \dots + \frac{\partial N_6}{\partial x} u_6 \\ \frac{\partial N_1}{\partial y} v_1 + \frac{\partial N_2}{\partial y} v_2 + \dots + \frac{\partial N_6}{\partial y} v_6 \\ \frac{\partial N_1}{\partial y} u_1 + \frac{\partial N_1}{\partial x} v_1 + \dots + \frac{\partial N_6}{\partial y} u_6 + \frac{\partial N_6}{\partial x} v_6 \end{array} \right\} \quad (2.39)$$

and in the matrix form

$$\xi = \left[\begin{array}{cccccc} \frac{\partial N_1}{\partial x} & 0 & \frac{\partial N_2}{\partial x} & 0 & \dots & \frac{\partial N_6}{\partial x} & 0 \\ 0 & \frac{\partial N_1}{\partial y} & 0 & \frac{\partial N_2}{\partial y} & \dots & 0 & \frac{\partial N_6}{\partial y} \\ \frac{\partial N_1}{\partial y} & \frac{\partial N_1}{\partial x} & \frac{\partial N_2}{\partial y} & \frac{\partial N_2}{\partial x} & \dots & \frac{\partial N_6}{\partial y} & \frac{\partial N_6}{\partial x} \end{array} \right] \left\{ \begin{array}{l} u_1 \\ v_1 \\ u_2 \\ v_2 \\ \vdots \\ u_6 \\ v_6 \end{array} \right\} \quad (2.40)$$

and therefore,

$$\xi = B \delta \quad (2.41)$$

in which

$$B = [B_1, \dots] = [B_1, B_2, \dots, B_6] \quad (2.42)$$

In which B is strain-displacement transformation matrix, which consists of the derivatives of shape functions with respect to x and y coordinates.

δ is nodal displacements vector as,

$$\delta = [u_1, v_1, \dots, u_6, v_6]^T \quad (2.43)$$

Strain vector in equation (2.30) can be also expressed as,

$$\xi = B \delta = [B_1, \dots, B_6] [\delta_1, \dots, \delta_6]^T$$

In which

$$B_i = \begin{bmatrix} \frac{\partial N_i}{\partial x} & 0 \\ 0 & \frac{\partial N_i}{\partial y} \\ \frac{\partial N_i}{\partial y} & \frac{\partial N_i}{\partial x} \end{bmatrix} \quad (2.44)$$

and

$$\delta_i = [u_i, v_i]^T \quad (2.45)$$

To be able to evaluate the stiffness matrix of an element, we need to calculate the strain-displacement transformation matrix. The element strains are obtained in terms of derivatives of element displacements with respect to general coordinates x and y . Because the element displacements are defined in natural coordinates system using equation (2.26) we need to relate the x -and y -derivatives to the H -and S -derivatives, where we realize that equation (2.25) is of the form

$$\begin{aligned} x &= f_1(H, S) \\ y &= f_2(H, S) \end{aligned} \quad (2.46)$$

where f_i denotes function of. The inverse relationship is

$$\begin{aligned} H &= f_3(x, y) \\ S &= f_4(x, y) \end{aligned} \quad (2.47)$$

We require the derivatives

$\frac{\partial}{\partial x}$ and $\frac{\partial}{\partial y}$, and it seems natural to use chain rule in the following form:

$$\frac{\partial}{\partial x} = \frac{\partial}{\partial H} \frac{\partial H}{\partial x} + \frac{\partial}{\partial S} \frac{\partial S}{\partial x} \quad (2.48)$$

with similar relationship for $\frac{\partial}{\partial y}$.

However, to evaluate $\frac{\partial}{\partial \mathbf{x}}$ in equation (2.48) we need to calculate

$$\frac{\partial H}{\partial \mathbf{x}} \quad \text{and} \quad \frac{\partial S}{\partial \mathbf{x}},$$

which means that the explicit inverse relationship in equation (2.47) would need to be evaluated. These inverse relationships are in general difficult to establish explicitly, and it is necessary to evaluate the required derivatives in the following way. Using the chain rule, we have

$$\begin{bmatrix} \frac{\partial}{\partial H} \\ \frac{\partial}{\partial S} \end{bmatrix} = \begin{bmatrix} \frac{\partial \mathbf{x}}{\partial H} & \frac{\partial \mathbf{y}}{\partial H} \\ \frac{\partial \mathbf{x}}{\partial S} & \frac{\partial \mathbf{y}}{\partial S} \end{bmatrix} \begin{bmatrix} \frac{\partial}{\partial \mathbf{x}} \\ \frac{\partial}{\partial \mathbf{y}} \end{bmatrix} \quad (2.49)$$

or in matrix notation

$$\left\{ \frac{\partial}{\partial H} \right\} = |J| \left\{ \frac{\partial}{\partial \mathbf{x}} \right\} \quad (2.50)$$

Where J is the jacobian operator relating the natural coordinate to general coordinate derivatives. We should note that jacobian operator can easily be found using equation (2.25).

$$\mathbf{x} = \sum_{i=1}^n N_i x_i$$

$$\mathbf{y} = \sum_{i=1}^n N_i y_i$$

$$J = \begin{bmatrix} \frac{\partial \mathbf{x}}{\partial H} & \frac{\partial \mathbf{y}}{\partial H} \\ \frac{\partial \mathbf{x}}{\partial S} & \frac{\partial \mathbf{y}}{\partial S} \end{bmatrix} = \begin{bmatrix} \frac{\partial N_1}{\partial H}, \frac{\partial N_2}{\partial H}, \dots \\ \frac{\partial N_1}{\partial S}, \frac{\partial N_2}{\partial S}, \dots \end{bmatrix} \begin{bmatrix} x_1 & y_1 \\ x_2 & y_2 \\ \vdots & \vdots \end{bmatrix} \quad (2.51)$$

In which

$$\frac{\partial N_1}{\partial H} = \frac{\partial}{\partial H} (\psi \Omega [1, 0, 0, 0, 0, 0]^T) = \psi_{,H} \Omega [1, 0, 0, 0, 0, 0]^T$$

$$\frac{\partial N_2}{\partial H} = \frac{\partial}{\partial H} (\psi \Omega [0, 1, 0, 0, 0, 0]^T) = \psi_{,H} \Omega [0, 1, 0, 0, 0, 0]^T$$

In which

$$\psi_{,H} = \frac{\partial \psi}{\partial H} \quad (2.52)$$

The variables vector ψ in equation (2.30) and the matrix of constants Ω in equation (2.32) are given

We require $\frac{\partial}{\partial x}$ and use

$$\frac{\partial}{\partial x} = |J^{-1}| \frac{\partial}{\partial H} \quad (2.53)$$

which requires that the inverse of J exists. This inverse exists provided that there is one-to-one correspondence between the natural and the local coordinates of the element, as expressed in equation (2.46), (2.47)

From equation (2.51)

$$\frac{\partial N_i}{\partial x} = [1, 0] |J^{-1}| \left\{ \begin{array}{c} \frac{\partial N_i}{\partial H} \\ \frac{\partial N_i}{\partial S} \end{array} \right\}$$

$$\frac{\partial N_i}{\partial y} = [0, 1] |J^{-1}| \left\{ \begin{array}{c} \frac{\partial N_i}{\partial H} \\ \frac{\partial N_i}{\partial S} \end{array} \right\}$$

After derivatives of the shape functions N_i with respect to x and y coordinates, we can construct the matrix B_i in equation (2.44) and from that the matrix B in equation (2.42)

From equation (2.24) the stiffness matrix is,

$$K = \int B^T D B dV \quad (2.54)$$

We can calculate the element stiffness matrix K by integrating the variables coordinates H and S from 0 to 1 on the plane triangular element.

Having calculated matrixes K of individual elements into which the body is subdivided, the next step is to assemble these to form what is called the "overall stiffness matrix" or "system stiffness matrix" for the entire discretized domain of problem. This is done by ensuring that equilibrium and compatibility conditions are satisfied at all the nodes within the discretized domain.



CHAPTER III

3. CONSTRUCTING THEORETICAL MODEL

3.1. FINITE ELEMENT MODEL OF THE PROBLEM FOR STRESS ANALYSIS

The general arrangement of the transverse fillet weld joint investigated is shown in figure (3.1)

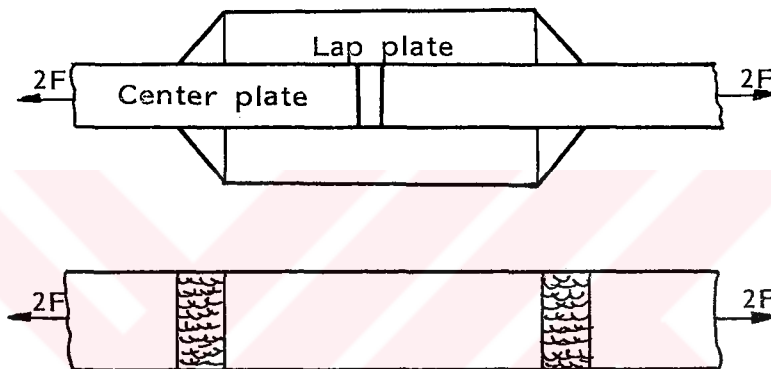


Figure: 3.1. The general arrangement of the transverse fillet weld joint investigated

In the present study, the thickness of center plates and lap plates are taken as equal. The thickness of plates is defined by h , legs of the fillet weld have the same length and are equal to h , l defines the length of weld.

The joint analysed is subjected to an axial tensile force $2F$. Thus the problem has symmetry with respect to loading condition and geometric properties. On account of the symmetry, only a quarter of the joint, which is shaded, was analysed as indicated in figure (3.2).

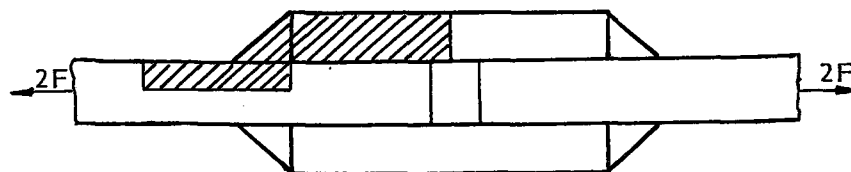


Figure: 3.2. A quarter of the joint which is shaded analysed

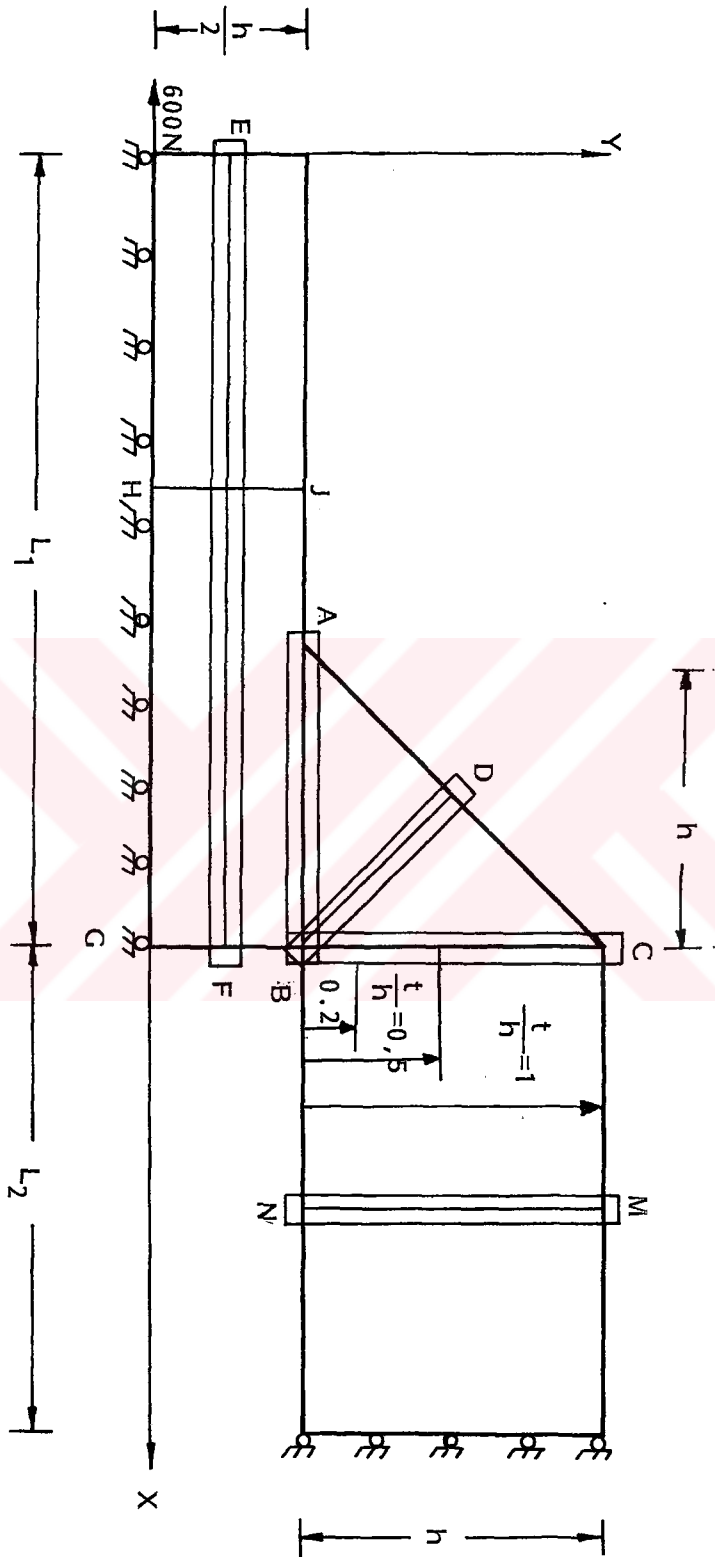


Figure: 3.3. Different directions of the model on which stresses distributions investigated

The joint has also the symmetric section on every vertical plane cutting it, we can treat the problem as the plane stress problem, by taking weld length of unit, which corresponds to thickness of the plane. Under the light of these specifications, we can construct the finite element model of the problem as shown in figure (3.3)

3.1.1. Boundary Conditions

It can be observed that, in the problem, the points on the middle line, x-axis, of the center plate have no vertical displacements. Hence we can put the sliding supports at the points on the x-axis as shown in figure (3.3). Again, the points on vertical line through center of the lap plate will not have horizontal displacements, thus we can also put the sliding supports on the vertical line as shown in figure (3.3). Thus we can shortly express the boundary conditions as follows:

- 1- The vertical displacement v of any point is zero if its y -coordinate is zero (see figure 3.3)

so we have

$$v = 0 \quad \text{if} \quad y = 0$$

- 2- The horizontal displacement u of any point is zero if its x -coordinate is equal to $L_1 + L_2$ (see figure 3.3)

so we have

$$u = 0 \quad \text{if} \quad x = 0$$

3.1.2. Mesh Generation

The plane domain of the problem is subdivided into plane triangular finite elements in computer with respect to the certain specification. It is obtained coordinate matrix of the nodal points and elements matrix consisting of numbers of the nodes to which is connected the individual element for calculation of the element stiffness matrixes. (see figure 3.4).

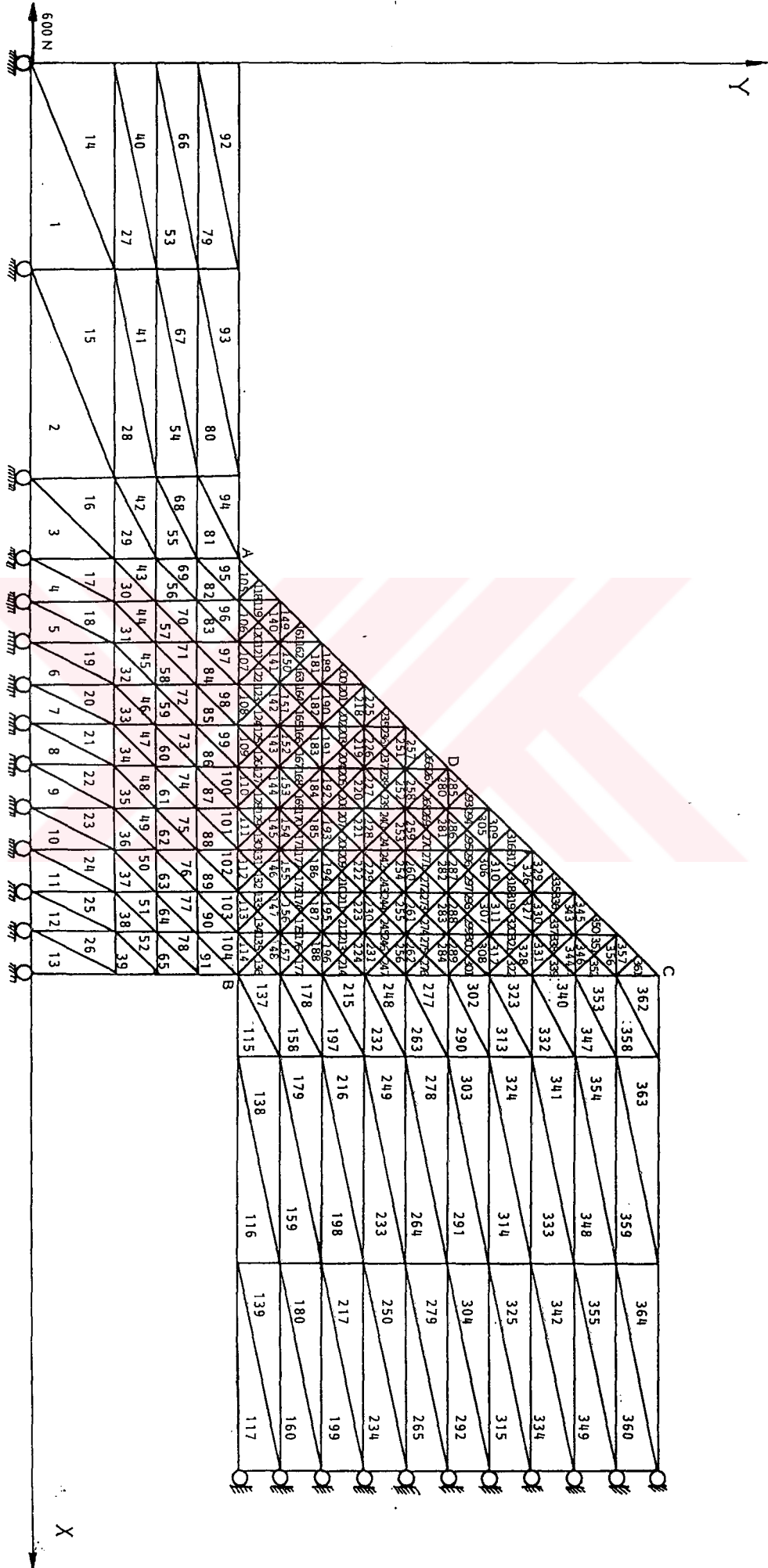


FIGURE: 3.4. THE FINITE ELEMENT MODEL OF THE SYMMETRIC QUARTER OF THE JOINT INVESTIGATED

3.2. DISPLACEMENT-STRAIN RELATIONS IN PLANE

In the plane, displacement strain relations are given as

$$\begin{aligned}\epsilon_x &= \frac{\partial u}{\partial x}, \\ \epsilon_y &= \frac{\partial v}{\partial y}, \\ \gamma_{xy} &= \frac{\partial u}{\partial y} + \frac{\partial v}{\partial x}\end{aligned}\quad (3.1)$$

3.3 STRESS-STRAIN RELATIONSHIPS

In the study, we shall assume that the material of the body is linearly elastic, isotropic and homogeneous, so that its elastic properties are completely specified by mutually independent constants E and ν , denoting elasticity modulus and Poisson's ratio respectively.

Stress-strain relationship in the plane is defined as (Hooke's law)

$$\sigma = D\xi \quad (3.2)$$

In which D is the elasticity matrix for plane stress in an isotropic material we have, by definition

$$\begin{aligned}\epsilon_x &= \frac{\sigma_x}{E} - \frac{\nu\sigma_y}{E} \\ \epsilon_y &= -\frac{\nu\sigma_x}{E} + \frac{\sigma_y}{E} \\ \gamma_{xy} &= \frac{2(1+\nu)}{E} \tau_{xy}\end{aligned}\quad (3.3)$$

Solving the above for the stress, we obtain matrix D as

$$D = \frac{E}{1-\nu^2} \begin{bmatrix} 1 & \nu & 0 \\ \nu & 0 & 0 \\ 0 & 0 & \frac{(1-\nu)}{2} \end{bmatrix} \quad (3.4)$$

in which E is the elastic modulus and ν is the Poisson's ratio.

3.4. MATERIAL PROPERTIES

In the present study, the material of the weld metal and material of the welded plates, lap and center plates, are the same, and isotropic one. So we have used the elasticity matrix for plane stress of isotropic material given in equation (3.4).

3.5. THE NUMERICAL VALUES USED IN THE STUDY

In the calculations, geometric dimensions are taken as

$$h = 15 \text{ mm}$$

$$L_1 = 4h$$

$$L_2 = 5h$$

The material properties are

$$\text{Elasticity modulus } E : 210 \text{ GPa}$$

$$\text{Poisson's ratio } \nu : 0.3$$

$$\text{The axial force } F : 600 \text{ N}$$

CHAPTER IV

4. RESULTS AND DISCUSSION

Plane stresses components σ_x , σ_y and τ_{xy} are calculated using finite element method; and principal stresses σ_1 , σ_2 and maximum shear stress τ_{max} from them, in computer by APL programming language.

Using the numerical values of stresses from computer, the distribution of each components of plane stress state σ_x , σ_y and τ_{xy} ; and also principal stresses σ_1 , σ_2 and maximum shear stress τ_{max} is plotted, in non-dimensional stress coordinate axis versus length coordinate axis, for every direction under consideration in the weld metal and welded plates. Non-dimensional coordinates of stress η and length χ are determined by dividing the stress calculated and distance interested by nominal stress σ_0 and the thickness of the plate h respectively. Nominal stress is equal to $\frac{F}{hI}$.

4.1. THE STRESS DISTRIBUTION IN WELD METAL

It is interesting to consider the variations of stresses on the weld legs AB and BC and throat of the weld DB figure (3.3).

4.1.1. The Stress Distribution On The Weld Leg BC

The distributions of stresses σ_x , σ_y , τ_{xy} , σ_1 , σ_2 and τ_{max} are shown in figure (4.1), (4.2) and (4.3). On the leg BC the maximum values of the all stresses occur at the point B. The value of the maximum principal stress σ_1 reaches approximately, 3 times of the nominal stress σ_0 . Evaluated value of σ_1 is $2.98\sigma_0$ at the point B, approximately. Minimum principal stress σ_2 occurs as compression stress, and its maximum value is calculated as $1.86\sigma_0$.

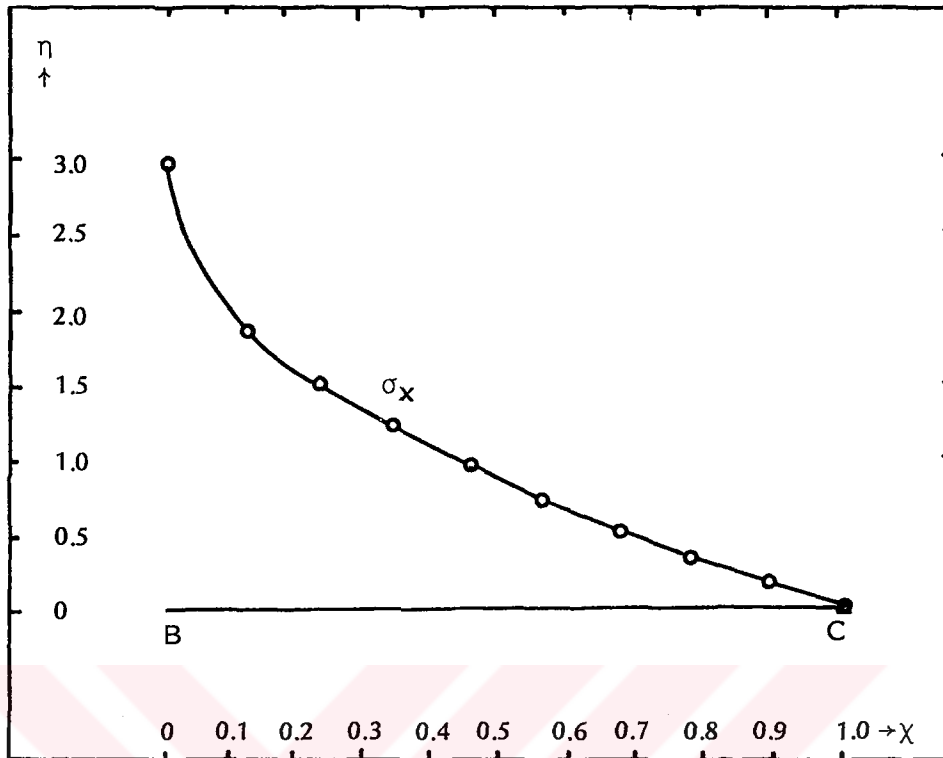


Figure: 4.1. Normal stress distribution on the leg BC

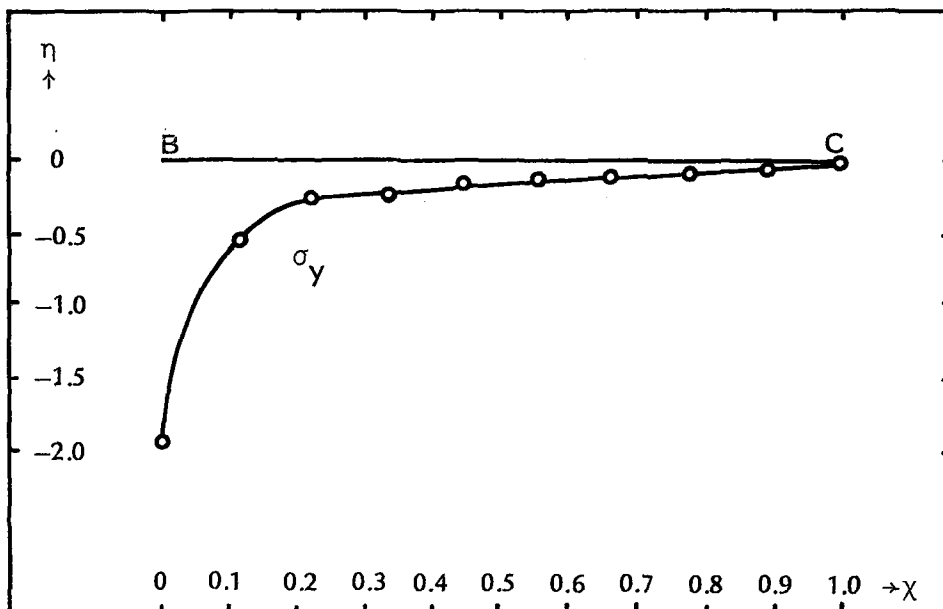


Figure: 4.2. Normal stress distribution on the leg BC

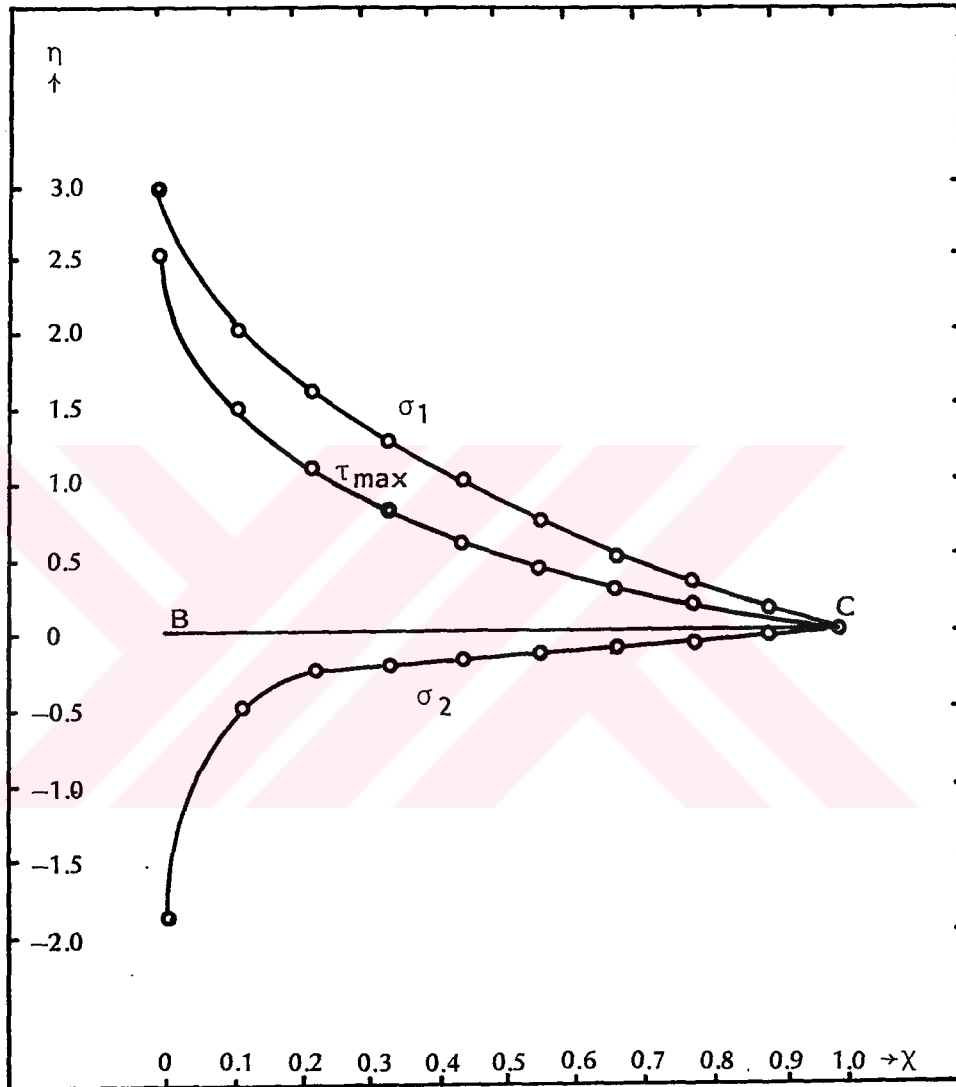


Figure: 4.3. Distributions of the principal stresses and max shear stress on the leg BC

4.1.2. The Stress Distribution On The Weld Leg AB

The distributions of the stress components are illustrated in figure (4.3), (4.4) and (4.5). It is observed maximum stress σ_1 occurs at the point A, the value of which reaches 5.5 times nominal stress σ_0 (see figure 4.6).



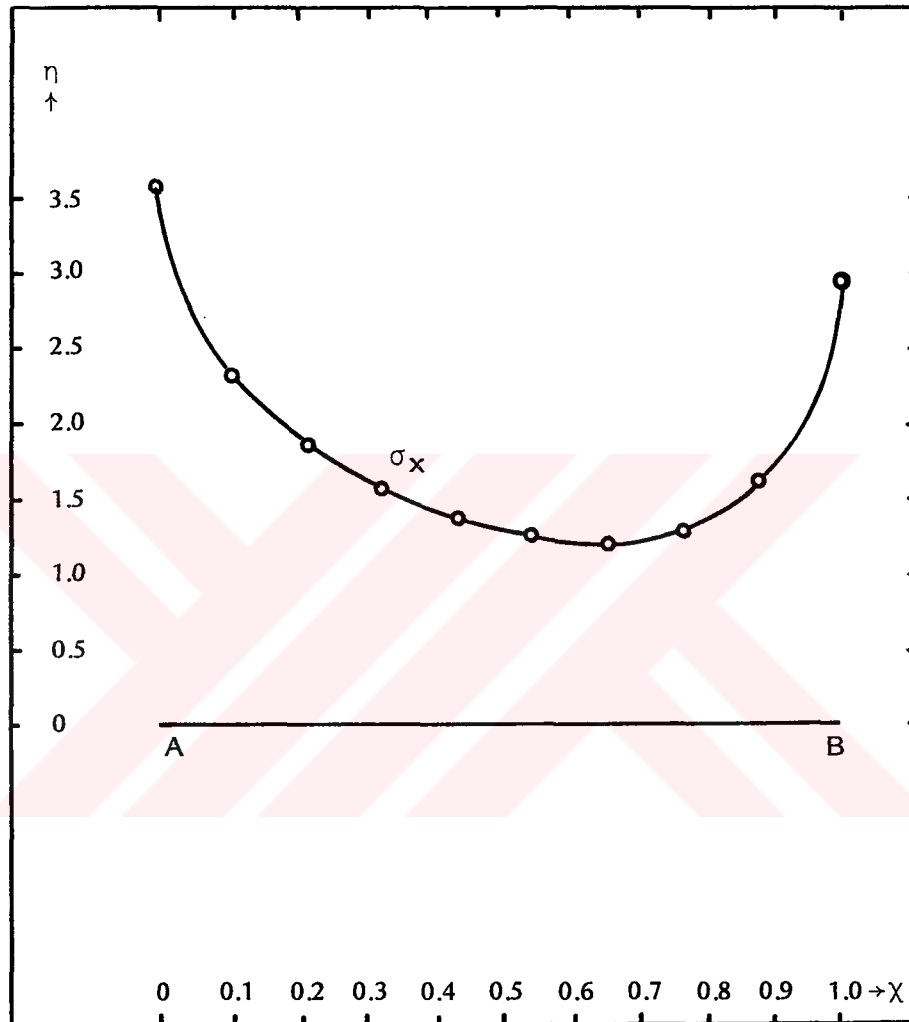


Figure: 4.4. Normal stress distribution on the leg AB

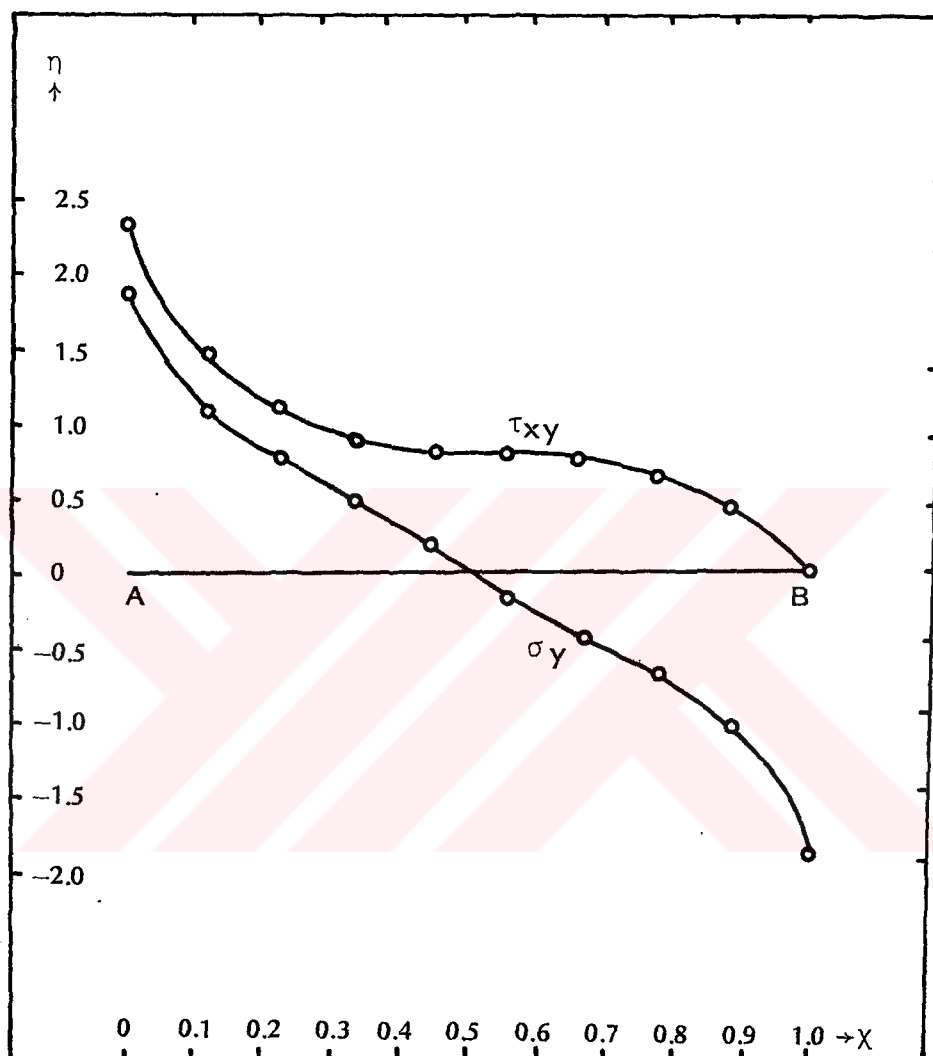


Figure: 4.5. Distributions of normal stress and shear stress on the leg AB

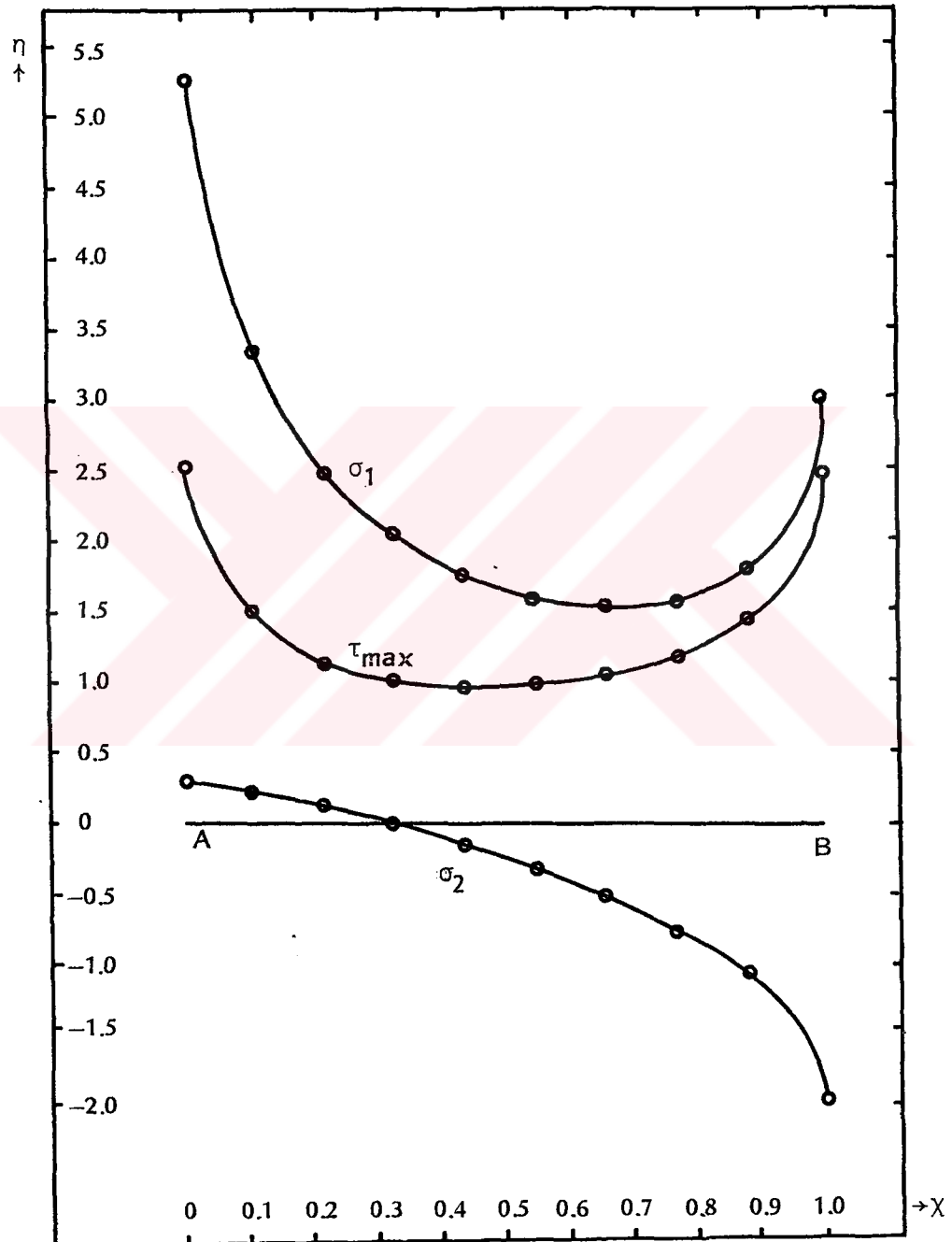


Figure: 4.6. Distributions of principal stresses and maximum shear stress on the leg AB

4.1.3. The Stresses Across The Throat DB Of The Weld

All stresses except τ_{xy} on the BD take their maximum values at the point B. Maximum value of σ_1 at the B is $1.98\sigma_0$ as stated in the explanation of stress on the BC. The shear stress τ_{xy} approaches zero at the B while the value of τ_{max} approaches that of the principal stress σ_1 at the point B. These graphs are shown in figure (4.7), (4.8) and (4.9).



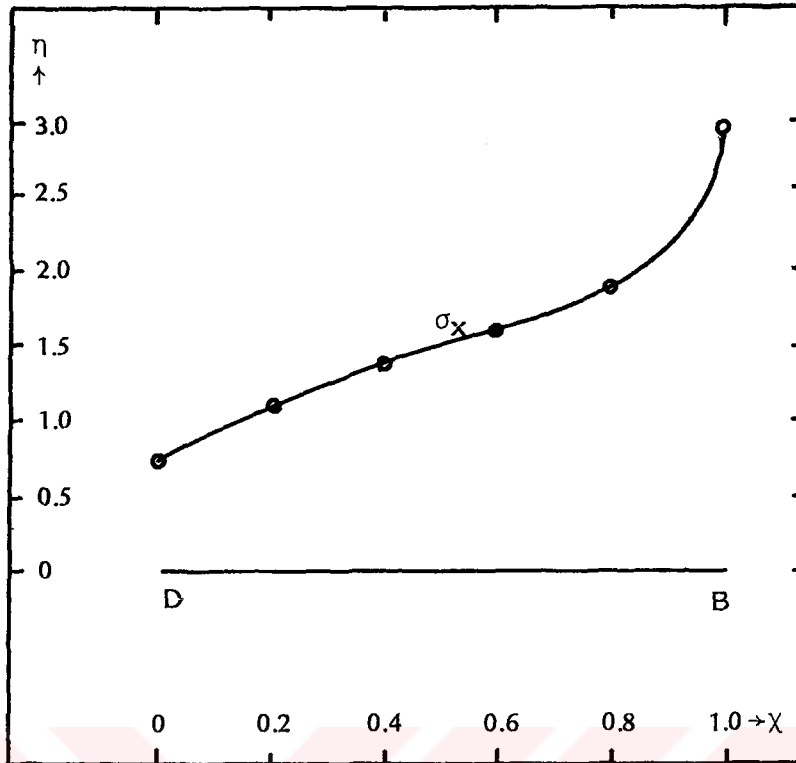


Figure: 4.7. Normal stress distribution on the troath DB of the weld

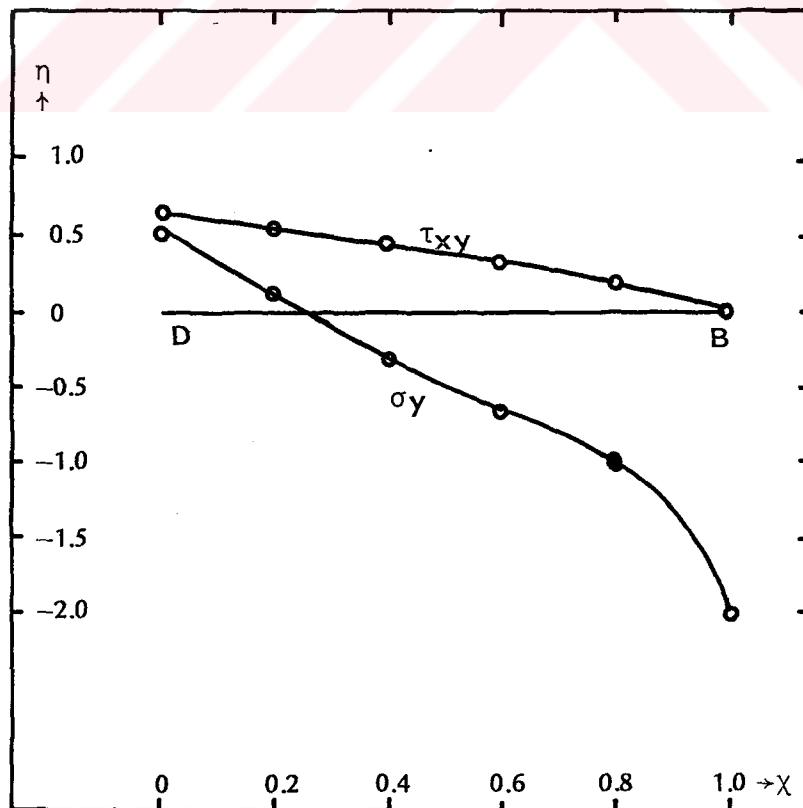


Figure: 4.8. Distributions of normal stress and shear stress on the troath DB of the weld

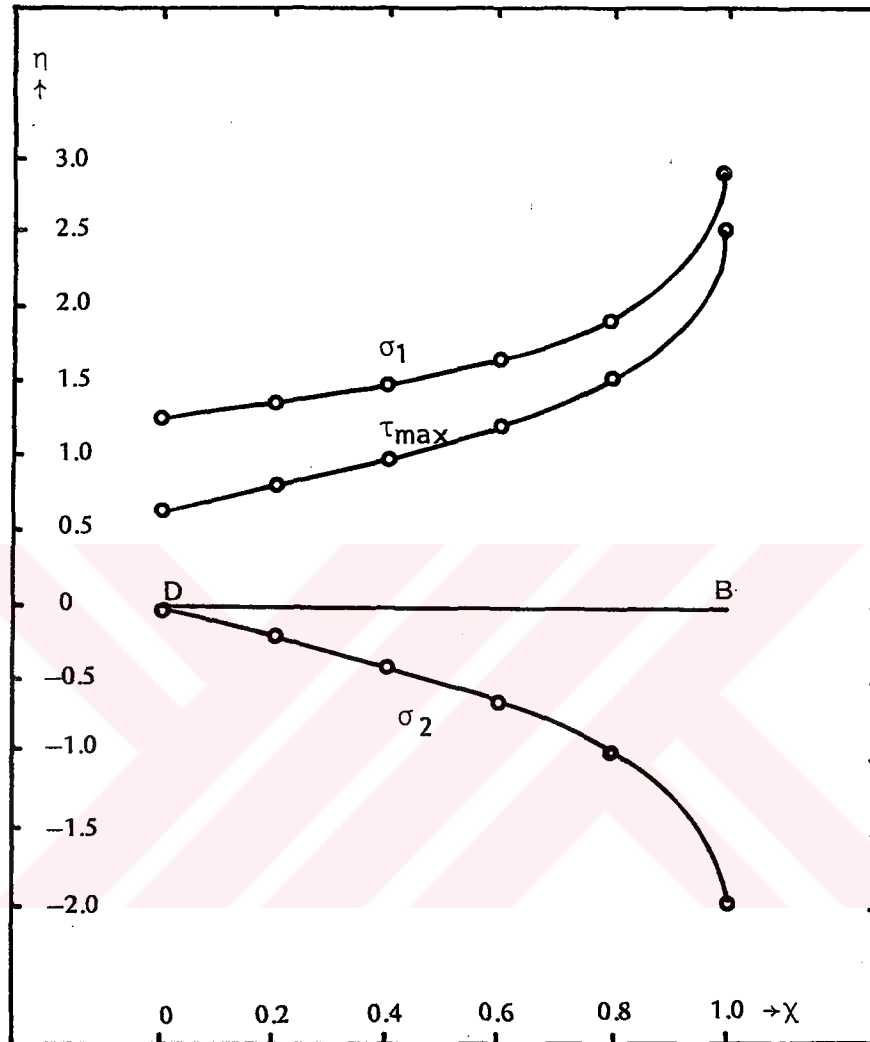


Figure: 4.9. Distributions of the principal stresses and maximum shear stress on the troath DB of weld

4.2. THE DISTRIBUTIONS OF THE STRESSES IN THE WELDED PLATES

As the legs AB and BC are adjacent to center plate and lap plate respectively, and also, the material of the weld metal and material of the plates are assumed as the same, the figure (4.1), (4.2) and (4.3) show stress distribution on the BC of lap plate as well as the leg BC of the weld metal. Again, the figure (4.4), (4.5) and (4.6) also show the distribution on the AB of the center plate.

4.2.1. The stresses In The Center Plate

Distributions of stresses σ_x , σ_y and τ_{xy} along the EF, which is taken in the middle thickness of the center plate, the E point is at $5h$ -distance from the plate end and the point F is on the end as shown in figure (4.3), are shown in figure (4.10), (4.11) and (4.12). It is note that the stress σ_x is constant until the point under the point on the EF. After that, the σ_x increases and reaches the zero at the point F. It is also remarkable that the stress σ_y is zero at the point E, which is $5h$ distance from the point F, and increases until $\chi=4$ and decrease after $\chi=4$ and takes zero at the $\chi=4$ and maximum negative value of the point F. In left hand side of the point E in the plate we have only the stress σ_x equal to nominal stress σ'_0 of center plate. σ'_0 has the value of $\frac{2F}{hl}$.

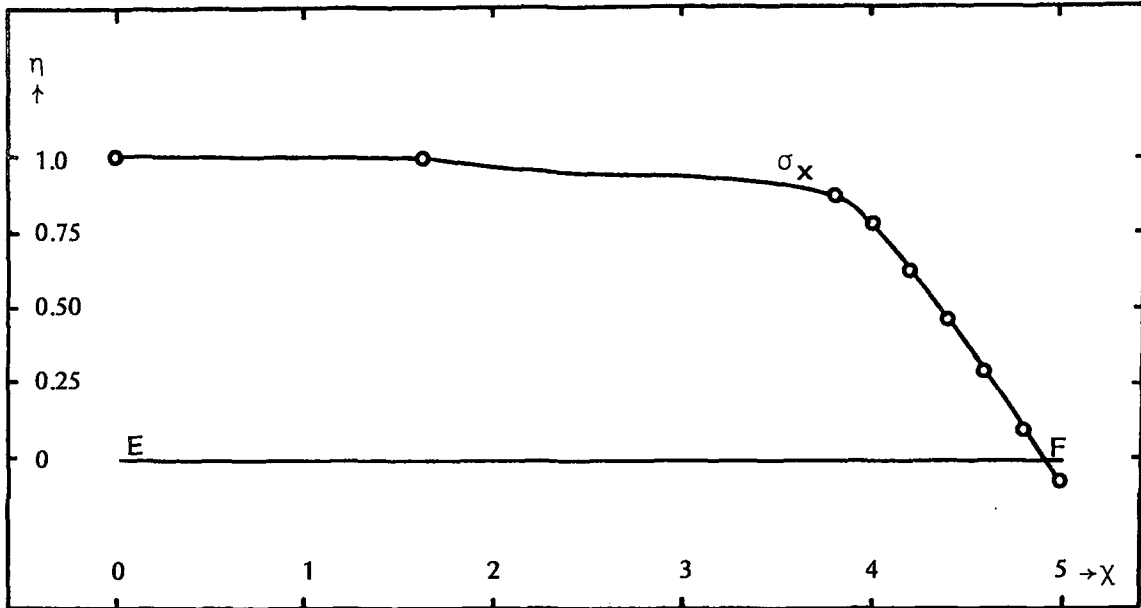


Figure: 4.10. Normal stress distribution on the EF in the center plate

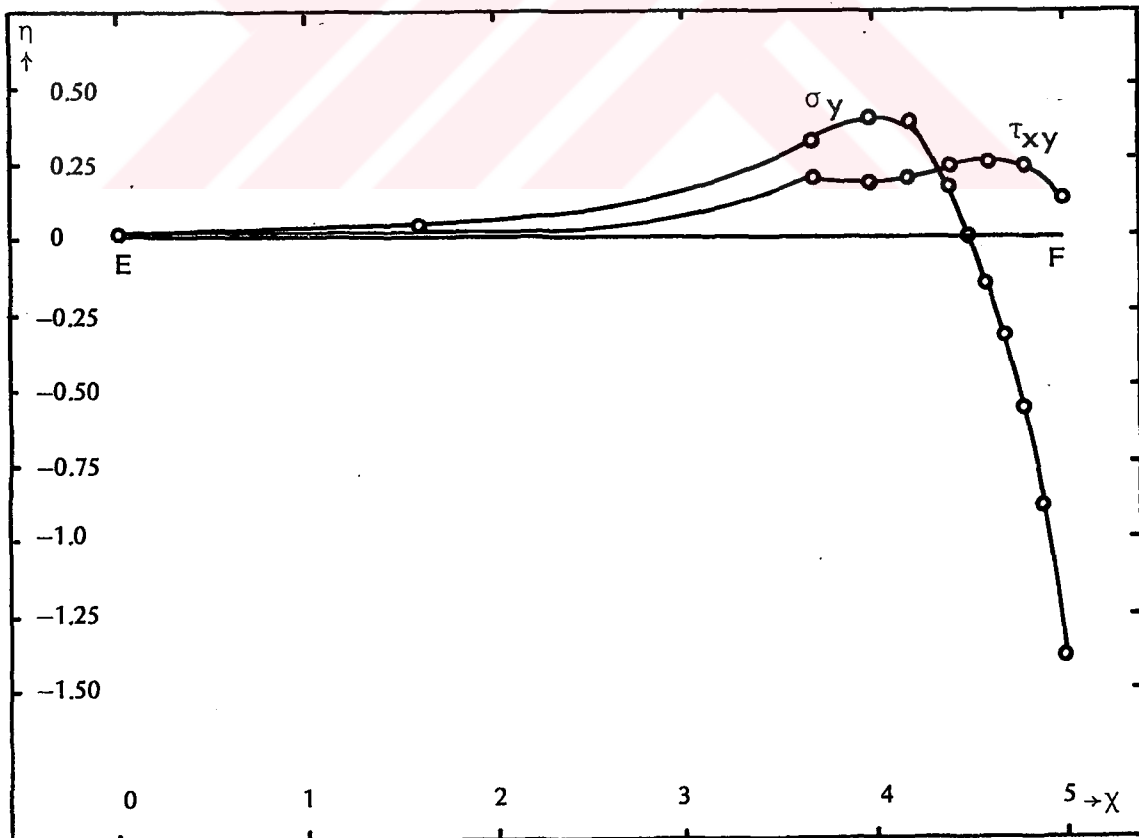


Figure: 4.11. Distributions of normal stress and shear stress on the EF in the center plate

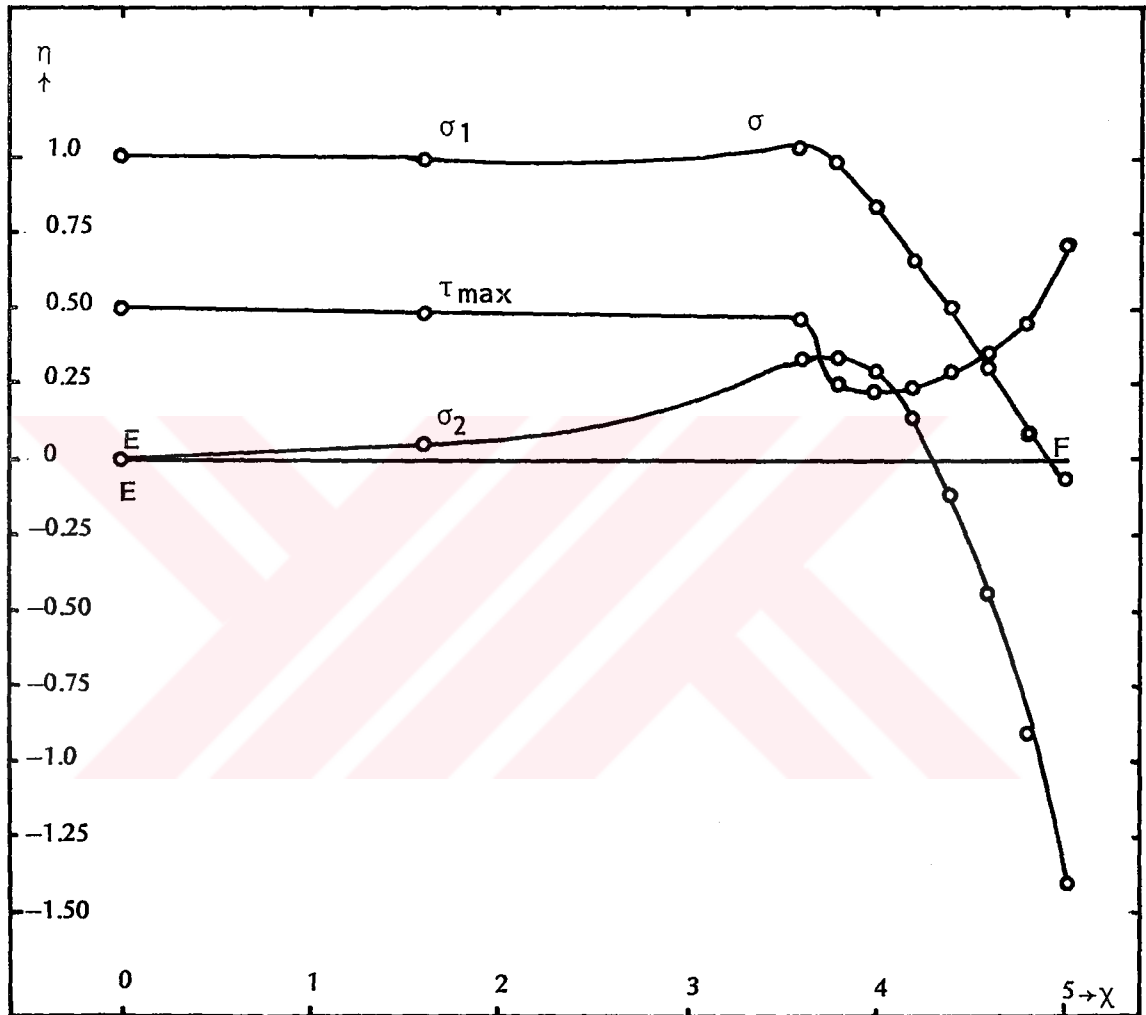


Figure: 4.12. Distributions of the principal stresses and maximum shear stress on the EF in the center plate

4.2.2. The Stresses In The Lap Plate

The lap plate in the joint, in fact is one of the additional plate parts used to make a fillet weld joint as shown in figure (3.1). As the weld leg BC is adjacent to lap plate left end the illustrations for the stresses distributions of the leg BC in figure (4.1), (4.2) and (4.3) represent also those of the lap plate.

Variation of σ_x -stress along the length of the lap plate is illustrated for t/h -ratios. It is remarkable that the σ_x -stresses for all $\frac{t}{h}$ ratios take uniform state after $\chi=1.5$ in which $\chi=l/h$. It is also observed that the σ_x has maximum value $3\sigma_0$ or $\eta=3$ for $t/h=0$ on $\chi=0$, which corresponds to the point B. It was observed the same value at the B ($\sigma_x=3\sigma_0$) in the figure (4.1) at the $\chi=0$ for $t/h=1$, σ_x is approximately zero, and it increases until 3 as the t/h ratio decreases. In figure (4.14). It is very interesting that in the middle of the lap plate $t/h=0.5$, σ_x -stress is equal to nominal stress σ_0 ($\chi=1$) and it does not change from $\chi=0$, to $\chi=4$ as seen in figure (4.14). At $\chi=0$, maximum σ_x occurring at $t/h=0$ and minimum σ_x occurring at $t/h=1$ close to the nominal stress value σ_0 as the χ increases and they maintain their uniform value after $\chi=1.5$. As seen in figure (4.14). The curves for σ_x upper ones and lower ones close to the stress value in the middle thickness $t/h=0.5$ as shown in the figure (4.14).

The stress distributions of stresses σ_x , σ_y and τ_{xy} on the MN across the lap plate are plotted in figure (4.13). In the MN section which is sufficient distance from the right of the lap plate, stresses σ_y and τ_{xy} , as it is expected should be zero and σ_x should be uniform and equal to σ_0 . The differences observed may arise from truncation and roundness errors in computer. They become smaller as the number of element or the nodes of individual element increase.

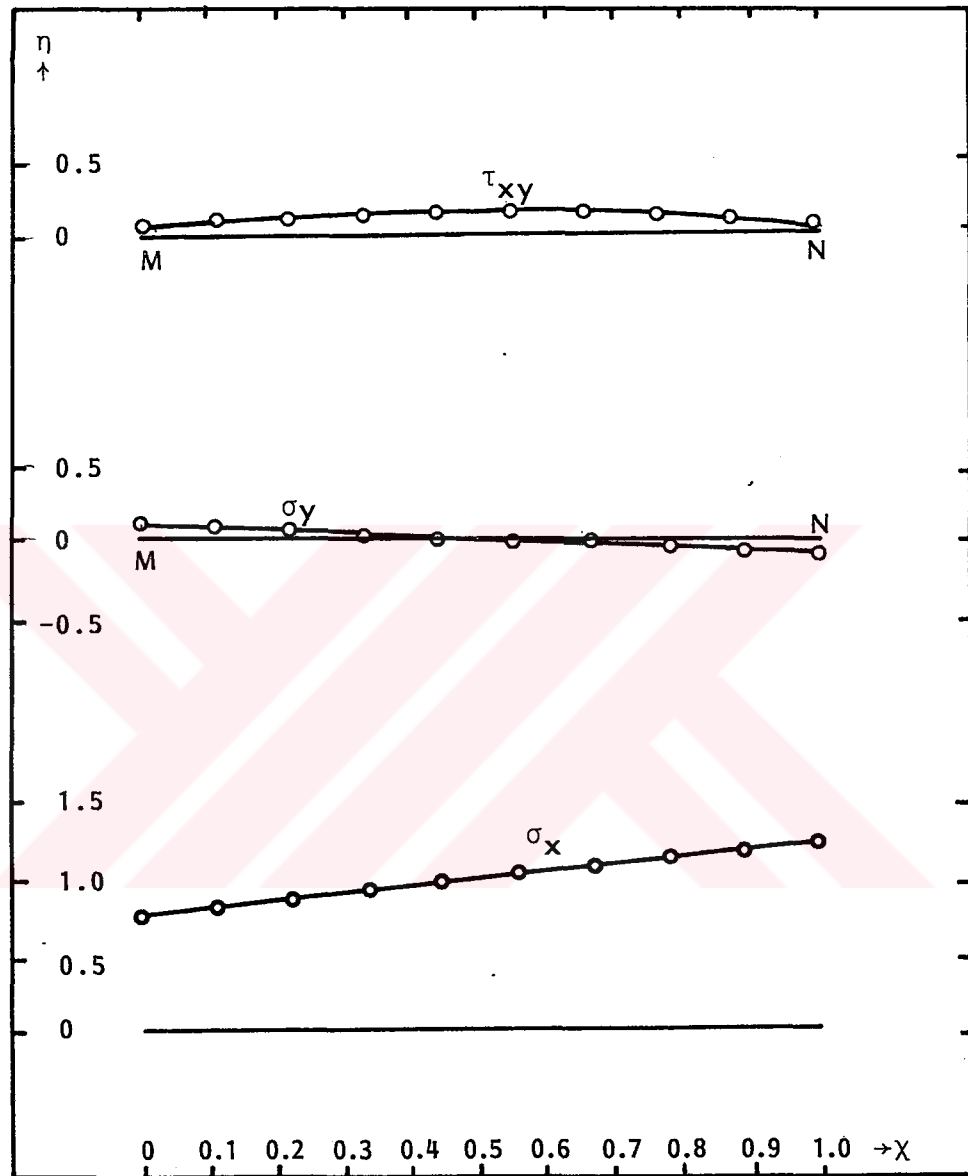


Figure: 4.13. Stresses distributions on MN in the lap plate

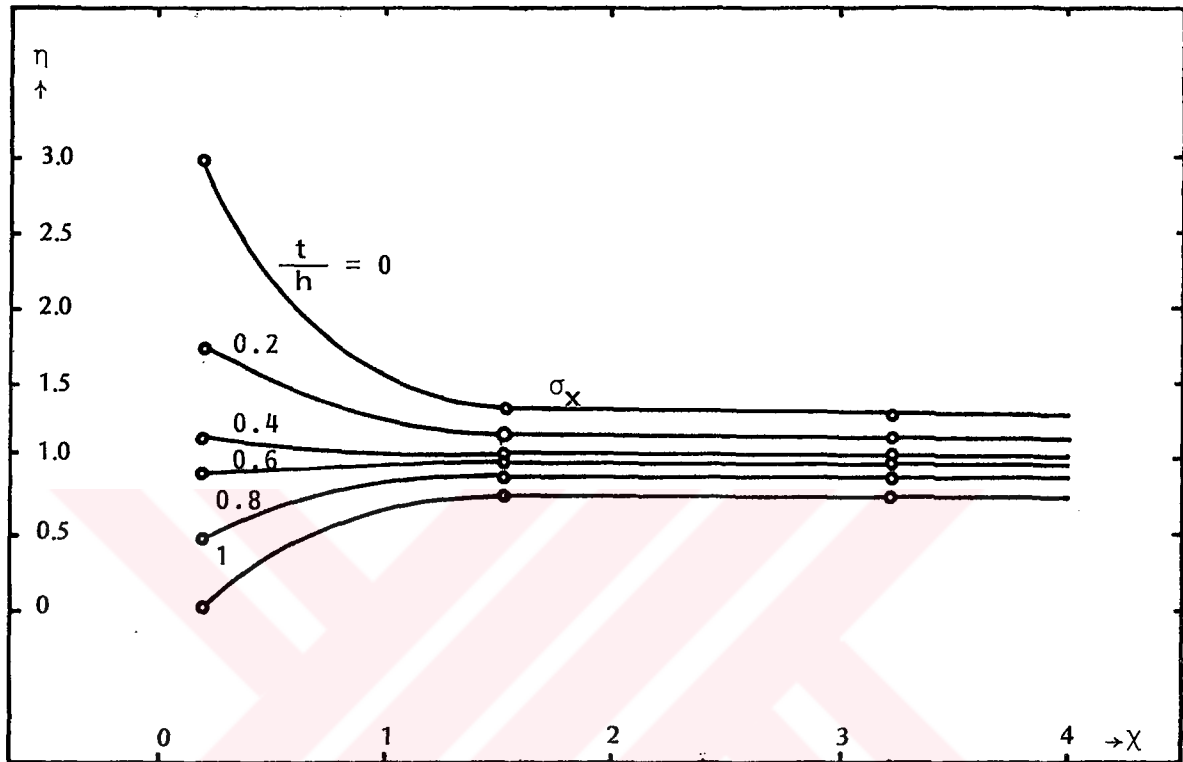


Figure: 4.14. The variation of the σ_x in different thicknesses along the length of the lap plate

E.N.	σ_x (MPa)	σ_y (MPa)
80	79.586	- 0.414
93	79.685	0.604
54	80.507	2.737
67	79.724	0.045
28	81.151	5.210
41	79.412	- 0.914
2	81.634	7.244
15	78.333	- 4.183

Table: 4.1. Some of the stresses values on the JH in the center plate

$$\sigma_o = \frac{\sum \sigma_x}{\sum n} = \frac{640.032}{8} = 80.004 \text{ MPa}$$

$$\sigma_o = \frac{F}{hl} = \frac{600}{7.5} = 80 \text{ MPa}$$

$$\text{error} : 80 - 80.004 = 0.004$$

$$\text{Percent} : \% 0.5$$

E.N: Numbers of elements.

CHAPTER V

CONCLUSIONS

In the light of the results obtained in this investigation it appears to be possible to draw the following conclusions.

In the weld, peak stresses occur at the points A, B, C and D. The biggest stress is $5.5\sigma_0$ at the point A approximately, $3\sigma_0$ at B, $1.25\sigma_0$ at D and zero stress at the point C, figure (4.3), (4.6) and (4.9).

Maximum shearing stresses in the weld occur at the point A and B, both of them is equal to $2.5\sigma_0$ approximately, figure (4.3) and (4.6).

In the weld, it appears also compression normal stresses, maximum absolute value of which occurs at the B equal to $2\sigma_0$, figure (4.3) and (4.6).

As the weld legs AB and BC are adjacent to center and lap plates, respectively, the distribution for AB and BC are also represent those of center and lap plates respectively, figure (4.1, 2, 3, 4, 5 and 6).

Stresses at points on the middle line of the center plane in the left hand side of HJ, figure (3.3) which is at the h -distance from the A, close to uniform values σ'_0 , $0.5\sigma'_0$ and zero σ_1 , τ_{\max} and σ_2 respectively, figure (4.11).

In the lap plate, stress in the part after h -distance from BC, close to uniform value; σ_x close to σ_0 , σ_y and τ_{xy} to zero, figure (4.13).

In the practice, average stress equation (1.1), value of which is $1.41\sigma_0$ is normally used in designing joints having fillet weld, but we have computed that maximum stress value occurring in the weld is approximately $5.5\sigma_0$ at the point A, so it is suggested that the equation used in designing, in practice, should be changed or the safety number is taken higher.

In the designing of dimensions, in practice, it is accepted that the element can be loaded until a stress at any point in it, reaches to yielding point of its material.

It might not be collapse the weld joint immediately, when plastic deformation begins at A, because the stress concentration reduces from A to B, so the problem should be studied from point of view of plastic analysis.

The results obtained have accuracy of 0.5 percent around exact value, as seen in table (4.1). Those stresses belong to the elements taken at a sufficient distance from the boundary end to eliminate the influence of loading (or boundary) condition, from point of view of Saint Venant's principle.



REFERENCES

1. Bathe, Klaus-Jürgen, "Finite Element Procedures in Engineering Analysis", 1982, by Prentice-Hall, Inc. Englewood Cliffs, New Jersey.
2. Blodgett, Omer W., "Allowables Enable Cost Reductions and the Use of Advanced Technologies in the Design of Structures and Weldments", *Welding Journal*, August 1970, 619-638.
3. Denayer, A., "Automatic Generation of Finite Element Meshes", *Computers and structures* 9, 359-364, 1978, Pergamon press, Britain.
4. Ghassemi, F., "Automatic Mesh Generation Scheme for a Two-or Three-Dimensional Triangular Curved Surface", *Computers and Structures* 15, 6, 613-626, 1982, Pergamon Press, Britain.
5. Gurney, T.R., "Some Finite Element Stress Analyses of Simulated Diffusion-Bonded Lap Joints", *Journal of Strain Analysis*, 12, 4, 1977, 331-338.
6. Günay, D. and Tekelioğlu, M., "Kompozit Tabakalı Dönen Delikli İnce Disklerde Optimum Gerilme Dağılımı", VI. Ulusal Mekânik Kongresi, 11-15 Eylül, 1989, Kirazlıyayla, Bursa.
7. Higgins, T.R. and Preece, F.R., "Proposed Working Stresses for Fillet Welds in Building Construction", *Welding Research Supplement*, 1968, 429-432.
8. Moser, K. and Swoboda, G., "Explicit Stiffness Matrix of the Linearly Varying Strain Triangular Element Computers and Structures 8, 311-314, 1978, Pergamon Press Britain.
9. Nath, B., "Fundamentals of Finite Elements for Engineers", The Athlone Press of the University of London, 1974.
10. Shighley, Joseph Edward and Mischke Charles, R., "Mechanical Engineering Design", Fifth Edition, 1989, Mc. Graw-Hill Inc.

11. Subramanian, G. and Bose, C.J., "Convenient Generation of Stiffness Matrices for the Family of Plane Triangular Elements", *Computers and Structures* 15, 85-89, 1982, Pergamon Press Britain.
12. Suzuki, Shin-Ichi, "Stress Analysis of Cemented Orthotropic Lap Joints", *Journal of Strain Analysis* 25, 1, 1990, 37-41.
13. Timoshenko, S., Goodier, J.N., Türkçesi: Kayan, I., Suhubi, E., "Elastisite Teorisi", Arı Kitabevi Matbaası, 1969.
14. Walsh, Richard Michael and Pipes, R. Byron, "Strain Energy Release Rate Determination of Stress Intensity Factors By Finite Element Methods", *Engineering Fracture Mechanics*, 22, 1, 17-33, 1985.
15. Zienkiewicz, O.C., "The Finite Element Method", Mc. Graw-Hill Book Co. UK, 1982.

APPENDIX

THE COMPUTER PROGRAMME

The general computer programme consists of four programmes. Three of them are main programmes and the other is subprogramme. The names of them are KKOOR, UCGEN, KAY and ASAL.

The programme ASAL is subprogramme of the KAY. By the programme KKOOR, the domain is subdivided into triangular elements; and the coordinates of the nodes connecting the elements are determined. This programme may make the mesh generation finer in desired level with respect to specifications.

The programme UCGEN denotes the nodes to which individual element connected as a matrix, dimensions of which are element number by number of nodes of individual element.

The programme KAY calculates stress components. The KAY runs when the numbers of elements and number of nodes are given. The KAY calculates the plane stress σ_x , σ_y and τ_{xy} . From these stresses, the ASAL-subprogramme included in the KAY computes the principal stresses σ_1 , σ_2 and maximum shear stress τ_{max} . The results obtained are recorded in SA in the programme ASAL when desired all values of stresses are taken as output in order σ_x , σ_y , τ_{xy} , σ_1 , σ_2 and τ_{max} . The values are in MPa.

:KK DDR_8'

*KKCOR; I; B; R2; W2; V; RR; RF2; WW2; ML; J; K; E S2; BB; II; RR1; WW1; ES1; JJ; KK; M2; W1; R1

'BIRINCI BÖLGE KAC EGRIDEN OLUSMAKTADIR'

I-16+/3B-,8

R2-W2-ES1-20

ET3:(? I), 'INCI EGRI ICIN M, N, A, E, E VE F DEGERLERINI GIRINIZ'

V-,8

(? I), 'INCI EGRI ICIN MAX R, MIN F VE F AFALIGINI GIRINIZ'

RR-,8

RR-(((3RR)83), 3)3RR

ES2-+/ES2-(RR_;1'-FR_;2')8FF_;3'

RR2-WW2-20

RF2-RR2, RR_1;2'6J-1

ET1:RR2-RR2, RR_J;2'+FF_;3'62(+.5+E S2_J')

|ET162(3ES2)DJ-J+16K-1

'EGRINIZ DOGRUSAL ISE (1), DAIRESEL ISE (2) GIRINIZ'

M1-8

I (M1=22)/ET2, ET12

ET12:W2-WW2, V_2'6(10.5-(-2))((26V_5'(RR2_K'))((RR2_K'+2)+(V_5'+2)-(V_6'

)))

|ET12(2(3RR2))>K-K+1

|E T22

ET2:W2-WW2, (V_1'6((V_3'(RR2_K')+V_4'))

|ET262(3RR2)>K-K+1

|ET22:R2-R2,-1.FF2

W2-W2,-1.WW2

ES1-ES1,ES2

|ET362B>I-I+1

R2-R2,-1CRR2

W2-W2,-1CWW2

'IKINCI BÖLGE KAC EGRIDEN OLUSMAKTADIR'

II-16+/3B-,8

R1-W1-ES1-20

ET6:(? II), 'INCI EGRI ICIN M, N, A, B, E VE F DEGERLERINI GIRINIZ'

V-,8

(? II), 'INCI EGRI ICIN MAX R, MIN R VE R ARALIGINI GIRINIZ'

RR-,8

RR-(((3RR)83), 3)3RR

ES1-+/ES1-(RR_;1'-RR_;2')8RR_;3'

RR1-WW1-20

RR1-RR1, RR_1;2'6JJ-1

ET4:RR1-RR1, RR_JJ;2'+RR_JJ;3'(2(+.5+ES1_JJ)'

|ET462(3ES1)DJ-JJ+16KK-1

'EGRINIZ DOGRUSAL ISE (1), DAIRESEL ISE (2) GIRINIZ'

M2-8

I (M2=22)/ET5, ET15

ET15:W1-WW1, V_2'6(1-2)((26V_5'(RR1_K'))((RR1_K'+2)+(V_5'+2)-(V_6'+2))

|ET15

|ET1562(3RR1)>KK-KK+1

ET25:R1-R1,-1.RR1

W1-W1,-1.WW1

ES1-ES1,ES1

|ET662RR>II-II+1

R1-R1,-1CRR1

W1-W1,-1CWW1

'CUS EY BÖLGE GRANLARINI GIRINIZ'

ES2-3OR-8

W-,1(0,+7(OR)7.6(W2-W1))

```

W1-(13W1)6L+ES2)3W1
W->(W+W)1
-k->1603,W
-w->20
-I->1
-E 135:
-I ET3662W_1'=(12)
-W->W
-I ET3562((ES1+1)6(ES2+1))>I->I+1
-ET36:=W_1'->0->W_1'
-I ET3562((ES1+1)6(ES2+1))>I->I+1
-k->k
R-((13R)6ES2+1)3R1
ES1->+/ES1
Z2->(3,DS)3(2DS-(ES1+1)6ES2+1),R,W
X->R
Y->W
Z1->((3,DS)3(2DS),X,Y
Z->Z1

```

```

:
ES <A Y DS K ;ALAN;G;P;X;Y;Z;I;II;III;J;K;KK;FF;BV;UV;G;M;P;E;SG
K-(2326ES)306 I->+/33ALAN-20
P->(ES,3,4)3C
L1:ALAN->ALAN,ODET(3,1311),3,23Z_D_I;1;2;3'
P->(-/Z_C_I;2;3';3'),(-/Z_C_I;3;1';3'),(430),(-/Z_D_I;3;2';2')
P->P,(-/Z_D_I;1;3';2'),(-/Z_C_I;3;2';2'),(-/Z_C_I;1;3';2')
P->P,(-/Z_D_I;2;3';3'),(-/Z_D_I;3;1';3')
G->(1' _I; ;')+. (C+. 6P_1; ;' -3 43P
X->(G_1;1'6A)+ (G_1;2'6B+|B|)+G_2;2'6C
Y->(G_1;3'6A)+(C_1;4'6B)+(G_2;3'6|B|)+G_2;4'6C
Z->(G_2;3'6A)+ (G_3;4'6B+|B|)+C_4;4'6C
K->(18ALAN_I' )6 (X, Y), _1' (|Y), Z
K->K_II;II->(23), _1.1'3+23'
K_II;II->K_II;II->((26C_I; ')-1), _1.1'26C_I; ''+K
|E162 ES>I->I+1
F->((26DS),1)3C
F_(-1+26(1 31 61 91 121 151 181)) ; I->-16((2.5 55 55 55 55 6 2.5)
EV->(26ES)3I-1
BV_(-1+26(30 60 70 120 150 180)),2((225) )->C
KK->BV /BV K
FF->BV F
UV->FF>KK
LV->V,UV
SG->(ES,3)30
E3:G->4 1306M->1
E2:G_M;'->L_M;' +.6Q+.6LV_II->(26D_I; ')-|EM<2; '
|E2624>M->M+1
SG_I; '-'>|(9ALAN_I') EC+. (P_I; ;' +. (G
|E362 ES>I->I+1
:
ASAL

```

```

:ASAL_&'
:
A SAL ;&PP ;S12;TOM;I
S12->TCM-206 I-1
E:S 12->S12,(.56+/SG_I;1 2') +1 -1((((.56-/SG_I;1 2')*2)+SG_I;3'*2)*0.5
TCM->TCM,0.56-/S12_((26I)-1),26I'
|E62((35C)_1')>I->I+1
&PP->3
SA->((ES,1)32E S), (SG), ((ES,2)ES 12), (ES,1) 3TOM
:

```

E.N	σ_x	σ_y	τ_{xy}	σ_1	σ_2	τ_{max}
1.000	88.873	-1.623	.173	88.873	-1.623	44.947
2.000	81.534	7.244	.629	81.640	7.238	37.200
3.000	63.791	35.845	5.369	64.080	29.656	17.662
4.000	50.936	32.054	7.240	52.200	27.720	12.705
5.000	44.141	25.859	8.346	47.375	23.623	11.075
6.000	37.743	20.396	9.067	41.617	16.522	12.543
7.000	31.364	11.493	10.030	35.527	7.230	16.202
8.000	24.832	.509	11.920	29.017	-3.675	16.346
9.000	18.239	-12.723	11.727	22.179	-16.664	15.471
10.000	12.025	-20.923	12.209	15.089	-32.206	23.937
11.000	7.253	-49.232	12.538	9.521	-51.699	30.670
12.000	3.407	-72.056	11.556	5.137	-73.786	39.461
13.000	4.257	-105.777	9.914	1.817	-104.652	56.245
14.000	81.489	5.497	33.335	94.040	-7.053	50.546
15.000	78.533	-4.183	.603	78.332	-4.182	41.259
16.000	66.546	2.717	8.981	67.786	1.478	33.154
17.000	54.902	23.178	6.727	57.449	23.580	15.050
18.000	49.700	29.684	6.350	51.544	27.839	11.853
19.000	44.507	26.969	4.601	45.604	25.812	9.928
20.000	39.316	23.777	3.691	39.734	20.059	9.338
21.000	31.259	12.902	3.062	33.602	11.565	15.957
22.000	26.551	1.925	2.265	26.750	.826	12.967
23.000	19.207	-12.345	.702	18.515	-12.345	17.928
24.000	12.286	-23.845	-2.268	12.410	-23.969	20.690
25.000	7.394	-47.101	-1.245	8.379	-47.101	23.717
26.000	5.110	-75.567	-11.573	6.737	-77.194	41.955
27.000	79.591	-1.263	.062	72.591	-1.263	40.222
28.000	81.151	5.210	1.555	81.133	5.178	38.000
29.000	75.247	31.712	19.612	82.777	24.183	28.299
30.000	56.027	31.928	17.393	65.137	22.818	21.159
31.000	45.199	28.022	17.241	57.941	18.372	25.235
32.000	42.595	21.597	17.460	52.234	10.958	20.638
33.000	34.152	11.231	19.262	47.799	1.284	23.100
34.000	29.579	.1402	19.363	39.234	-9.253	24.243
35.000	22.699	-21.249	22.332	32.142	-21.230	26.732
36.000	15.404	-25.999	20.785	24.038	-34.633	29.335
37.000	7.716	-46.272	19.624	14.263	-46.270	32.528
38.000	.598	-71.784	15.490	3.774	-74.960	39.357
39.000	6.294	-112.912	11.026	-4.968	-114.208	56.912
40.000	77.583	1.922	20.341	82.734	-3.200	42.952
41.000	79.412	-1.614	.967	79.623	-1.614	45.175
42.000	76.783	3.899	13.555	79.222	1.460	38.831
43.000	64.842	23.791	15.919	72.823	22.522	26.123
44.000	58.659	32.718	13.427	64.357	27.020	19.659
45.000	52.464	23.992	12.512	57.937	23.252	17.170
46.000	46.253	21.696	12.722	51.661	16.294	17.583
47.000	40.118	12.420	13.230	45.463	7.276	15.254
48.000	33.894	1.596	13.731	38.954	-3.364	21.159
49.000	27.239	-12.482	13.622	31.526	-14.771	23.169
50.000	19.624	-24.732	11.271	22.324	-27.432	24.373
51.000	13.789	-42.134	5.539	11.253	-43.620	27.432
52.000	8.282	-62.725	-4.246	8.535	-62.972	35.756
53.000	75.752	-1.846	-1.162	75.752	-1.847	38.950
54.000	80.507	2.737	1.002	80.523	2.724	38.898

E.N	σ_x	σ_y	τ_{xy}	σ_1	σ_2	τ_{max}
55.000	64.891	30.926	28.163	96.911	18.905	39.003
56.000	65.364	33.671	26.610	81.247	18.787	35.231
57.000	57.381	28.455	24.925	71.735	14.130	28.817
58.000	49.911	23.147	24.517	63.633	6.325	23.654
59.000	42.821	18.237	24.987	56.358	-3.300	29.829
60.000	35.143	-1.835	26.514	49.566	-14.264	35.918
61.000	29.522	-0.877	27.315	42.899	-26.255	34.577
62.000	22.623	-15.876	28.448	35.752	-39.662	37.285
63.000	14.962	-40.274	28.482	27.017	-52.330	39.672
64.000	5.161	-58.579	24.865	14.611	-67.020	40.819
65.000	-5.219	-117.726	16.125	-2.742	-110.202	53.730
66.000	75.550	.840	12.073	77.453	-1.062	35.237
67.000	79.724	.045	.878	79.734	.035	39.849
68.000	92.399	5.364	16.763	95.547	3.156	43.293
69.000	81.391	29.876	23.586	91.558	20.709	34.925
70.000	71.363	35.153	15.373	79.724	26.732	35.454
71.000	62.001	29.841	18.625	70.527	21.313	24.606
72.000	54.309	21.497	18.867	62.907	12.936	24.959
73.000	48.101	11.821	19.385	56.510	3.412	26.549
74.000	42.916	1.194	19.921	50.930	-6.739	28.443
75.000	38.188	-10.278	20.057	45.411	-17.500	21.456
76.000	33.523	-22.737	19.361	39.870	-28.224	22.697
77.000	25.515	-37.108	13.877	28.452	-40.046	34.249
78.000	22.443	-55.592	-2.368	12.521	-56.775	34.638
79.000	75.063	-.783	-.392	75.065	-.785	37.925
80.000	79.555	-1.414	-.905	79.594	-1.422	45.038
81.000	97.987	24.931	34.103	111.432	11.496	49.973
82.000	84.105	35.926	41.507	108.334	15.898	48.828
83.000	70.041	30.945	35.672	91.169	9.816	40.677
84.000	57.305	21.185	31.045	78.471	2.122	32.175
85.000	50.938	10.260	31.909	68.439	-7.241	37.843
86.000	44.371	-1.611	31.544	60.418	-17.939	28.149
87.000	38.291	-14.222	32.635	53.920	-29.851	41.885
88.000	33.019	-27.511	34.072	48.326	-42.859	45.572
89.000	27.433	-41.571	35.923	42.739	-56.877	49.808
90.000	19.982	-55.255	37.734	35.561	-71.159	53.351
91.000	7.128	-74.402	35.692	20.545	-87.819	54.182
92.000	74.747	.213	4.006	74.962	.600	37.481
93.000	79.685	.604	.656	79.691	.598	39.546
94.000	112.321	9.316	17.754	125.037	6.335	54.328
95.000	121.997	32.134	32.634	132.598	21.534	55.532
96.000	65.937	39.445	29.132	69.075	23.434	37.237
97.000	69.302	30.723	27.816	83.852	16.162	33.850
98.000	59.271	21.358	25.629	73.443	7.827	35.778
99.000	54.537	11.340	25.539	66.386	-.539	33.448
100.000	51.575	.542	25.037	61.035	-9.121	35.727
101.000	50.576	-10.506	24.740	59.428	-09.252	33.343
102.000	32.123	-21.772	23.946	52.230	-26.952	44.202
103.000	57.373	-32.599	21.455	62.228	-27.443	49.836
104.000	66.527	-41.467	19.725	67.978	-42.512	55.246
105.000	134.922	75.217	92.279	202.057	8.082	96.988
106.000	86.572	42.228	34.410	123.223	3.677	58.773
107.000	69.075	29.967	42.808	96.533	2.458	47.062
108.000	57.173	19.685	16.951	83.978	-3.137	42.542
109.000	53.220	5.949	33.516	70.810	-10.641	40.726

E.N	σ_x	σ_y	τ_{xy}	σ_1	σ_2	τ_{max}
110.000	49.888	-4.986	31.406	64.221	-19.320	41.771
111.000	48.815	-15.789	29.791	62.334	-28.229	44.232
112.000	50.412	-27.507	27.132	58.927	-26.004	47.475
113.000	56.419	-25.799	21.011	62.572	-40.361	56.657
114.000	71.741	-25.419	2.912	71.828	-25.806	48.667
115.000	115.255	18.110	-15.241	121.553	15.863	52.824
116.000	52.712	.404	-9.369	53.335	-.912	27.127
117.000	51.518	-.444	-8.287	52.955	-1.731	27.350
118.000	92.279	34.485	75.217	150.937	-4.172	77.584
119.000	75.876	69.564	55.242	119.624	5.836	58.884
120.000	78.118	38.996	51.237	113.422	3.713	54.844
121.000	64.553	24.556	47.655	94.975	4.639	45.166
122.000	66.453	26.472	41.161	92.221	.706	45.759
123.000	57.255	23.711	35.019	82.212	.769	39.731
124.000	59.295	14.067	35.637	78.888	-5.525	42.207
125.000	62.753	22.295	32.252	72.554	-5.891	38.133
126.000	55.005	1.511	32.533	70.374	-13.858	42.116
127.000	53.509	.192	29.926	64.515	-13.713	39.214
128.000	52.977	-10.974	30.716	65.340	-23.327	44.339
129.000	52.608	-11.679	27.938	61.247	-22.381	41.824
130.000	53.272	-23.042	29.232	63.001	-32.973	47.987
131.000	52.325	-22.866	25.125	62.825	-32.436	42.876
132.000	55.618	-33.771	26.848	63.051	-41.215	52.139
133.000	58.609	-22.574	19.282	61.479	-32.561	42.357
134.000	61.342	-40.748	21.007	65.496	-44.902	55.199
135.000	72.122	-27.214	5.714	72.417	-37.288	57.667
136.000	68.012	-13.126	5.216	68.346	-13.460	46.932
137.000	82.392	-9.412	10.441	84.032	-13.057	63.557
138.000	49.040	-2.955	5.780	49.675	-3.590	26.632
139.000	47.203	-.408	9.392	50.681	-2.726	24.256
140.000	67.321	46.332	52.168	112.040	3.613	53.213
141.000	62.231	31.451	41.008	92.510	2.982	43.758
142.000	57.373	19.080	34.805	77.950	-1.497	37.724
143.000	54.542	6.658	31.269	69.984	-8.776	39.979
144.000	53.699	-5.795	29.127	65.584	-17.681	41.633
145.000	54.715	-18.063	27.379	64.049	-17.239	41.524
146.000	58.534	-29.230	24.840	65.076	-35.773	50.425
147.000	64.541	-37.523	19.275	68.050	-41.263	54.532
148.000	69.393	-24.921	8.020	70.070	-25.598	47.834
149.000	72.435	54.716	61.373	122.321	1.821	61.757
150.000	64.192	38.665	49.439	102.489	.368	51.050
151.000	55.903	23.840	41.259	85.134	-3.553	44.059
152.000	55.585	10.142	35.683	75.166	-9.440	42.308
153.000	54.635	-2.690	31.511	69.565	-16.622	42.057
154.000	56.063	-14.168	27.441	65.513	-23.618	44.566
155.000	62.315	-22.278	21.074	65.697	-22.622	47.275
156.000	67.852	-26.486	12.485	69.476	-38.111	48.794
157.000	71.362	-15.356	1.619	71.391	-16.327	44.559
158.000	86.356	10.473	-10.082	87.673	9.137	39.258
159.000	52.543	.392	-8.324	51.403	-.265	25.126
160.000	48.294	-.439	-8.302	50.643	-1.789	25.216
161.000	61.373	41.485	55.714	112.046	-2.132	57.541
162.000	56.733	47.093	49.175	101.227	2.499	49.414
163.000	58.775	32.755	46.659	94.840	-2.311	46.276
164.000	54.060	31.041	40.600	84.750	.351	42.200

E.N	σ_x	σ_y	τ_{xy}	σ_1	σ_2	τ_{max}
165.000	56.808	18.084	39.171	81.141	-8.249	43.695
166.000	52.532	16.021	34.712	73.707	-4.573	39.549
167.000	55.203	4.211	33.984	72.192	-12.778	42.455
168.000	53.579	3.451	39.397	67.162	-11.041	39.190
169.000	55.213	-8.538	33.094	67.075	-20.499	43.837
170.000	54.630	-8.707	26.357	64.177	-18.234	41.205
171.000	55.942	-19.515	26.239	65.087	-27.653	46.355
172.000	53.665	-18.998	21.167	64.033	-24.352	44.226
173.000	60.413	-27.227	20.836	65.113	-31.928	48.521
174.000	64.769	-23.919	13.163	65.641	-27.791	47.216
175.000	64.731	-25.737	11.846	65.257	-27.263	46.750
176.000	62.553	-24.580	4.009	68.825	-24.733	46.772
177.000	65.643	-19.367	2.221	65.757	-10.432	38.070
178.000	63.214	-11.095	9.127	64.319	-12.225	35.259
179.000	47.179	-1.280	8.667	48.682	-2.784	25.735
180.000	46.949	-0.528	8.271	42.373	-1.571	25.172
181.000	52.316	41.184	46.399	93.481	.009	46.731
182.000	52.065	25.277	38.511	75.445	-2.125	43.774
183.000	52.151	19.870	23.012	70.445	-7.423	38.934
184.000	51.254	-2.398	28.968	65.590	-14.735	43.157
185.000	55.529	-14.054	25.148	63.666	-22.191	42.929
186.000	53.753	-22.947	20.129	62.448	-27.635	45.542
187.000	61.649	-25.170	12.525	63.419	-26.941	45.180
188.000	62.933	-15.370	4.620	63.291	-18.257	42.509
189.000	54.210	47.095	50.406	101.371	.334	50.518
190.000	51.675	30.643	42.312	86.091	-1.583	43.542
191.000	53.405	15.048	35.561	74.629	-6.177	40.403
192.000	54.389	1.388	29.947	67.272	-5.556	39.504
193.000	56.847	-9.659	24.362	64.817	-17.628	41.222
194.000	62.561	-16.939	17.662	64.397	-20.776	42.585
195.000	63.633	-18.554	9.719	64.767	-19.688	42.227
196.000	63.325	-13.596	3.029	63.944	-13.716	38.979
197.000	68.496	6.509	-6.511	69.172	5.832	31.670
198.000	47.681	.396	-8.284	49.390	-1.212	25.652
199.000	46.971	-0.436	-8.315	48.387	-1.852	25.120
200.000	50.605	40.487	47.495	93.299	-2.357	47.734
201.000	47.225	39.532	41.646	85.201	1.556	41.823
202.000	50.566	23.781	29.619	78.094	-6.557	41.229
203.000	43.122	23.048	34.830	72.602	-1.433	37.007
204.000	51.177	5.642	33.237	69.260	-9.568	39.459
205.000	49.952	8.274	29.282	65.053	-6.327	35.940
206.000	52.592	-4.177	27.559	64.050	-6.623	38.942
207.000	52.743	-4.130	23.979	61.503	-12.891	37.197
208.000	54.812	-13.805	22.677	61.522	-20.695	41.159
209.000	56.231	-13.459	17.893	60.556	-17.784	39.172
210.000	57.368	-18.521	16.297	66.708	-22.169	41.434
211.000	59.177	-13.278	10.845	60.656	-19.768	40.217
212.000	58.879	-16.876	8.591	55.959	-15.926	38.997
213.000	59.986	-16.544	4.857	60.293	-16.851	38.572
214.000	59.315	-8.664	2.075	58.438	-6.797	32.612
215.000	51.982	-10.564	6.921	52.739	-11.320	32.003
216.000	44.929	-0.804	15.121	46.077	-2.752	24.855
217.000	44.617	-0.523	8.382	46.123	-2.020	24.076
218.000	44.116	32.670	38.961	77.072	-0.981	35.179
219.000	45.895	16.641	32.505	66.912	-4.377	35.545

E.N	σ_x	σ_y	τ_{xy}	σ_1	σ_2	τ_{max}
220.000	48.154	2.711	27.300	60.951	-10.086	35.519
221.000	50.707	-9.356	22.295	58.177	-15.826	37.300
222.000	53.089	-15.342	16.526	56.822	-19.126	37.974
223.000	54.422	-16.600	10.037	55.808	-17.986	36.897
224.000	54.475	-11.512	4.701	54.808	-13.945	33.376
225.000	49.769	28.276	41.400	83.547	1.309	41.574
226.000	47.170	20.892	33.858	70.349	-2.287	36.318
227.000	47.279	6.461	27.516	62.734	-5.974	34.864
228.000	51.905	-4.359	21.540	59.206	-01.658	30.432
229.000	54.379	-11.903	15.311	57.783	-7.426	36.343
230.000	55.594	-12.694	9.157	56.801	-13.900	35.351
231.000	54.989	-13.237	4.554	55.805	-15.254	32.879
232.000	56.361	4.031	-4.114	56.682	3.710	26.486
233.000	45.120	1.406	-9.237	46.575	-1.677	29.833
234.000	44.544	-1.433	-8.327	46.134	-1.922	24.026
235.000	41.407	12.574	23.178	74.567	-2.777	28.559
236.000	39.765	30.084	33.376	68.650	1.199	33.726
237.000	42.151	16.123	30.953	62.924	-5.580	34.187
238.000	42.766	14.007	27.238	59.188	-2.414	30.800
239.000	45.384	1.098	25.056	56.779	-10.177	37.473
240.000	45.958	1.234	21.635	54.711	-7.520	31.116
241.000	47.931	-7.935	19.520	54.049	-13.993	34.206
242.000	48.763	-7.571	15.925	52.951	-11.761	32.356
243.000	49.712	-12.030	13.747	52.633	-14.977	33.616
244.000	50.455	-11.833	10.308	52.117	-13.494	32.826
245.000	52.354	-11.354	8.107	51.401	-12.400	31.900
246.000	50.536	-11.299	6.012	51.115	-11.878	31.497
247.000	49.554	-7.142	3.978	49.932	-7.419	28.674
248.000	42.996	-9.140	6.862	43.884	-10.028	26.956
249.000	42.789	-1.190	19.775	44.866	-2.767	23.817
250.000	42.313	-1.436	8.391	43.900	-2.024	22.963
251.000	35.747	27.315	16.472	63.631	-3.689	31.130
252.000	38.991	8.644	24.778	52.872	-5.238	29.065
253.000	41.733	-7.247	19.616	49.386	-9.696	28.541
254.000	44.103	-8.725	14.360	47.754	-12.376	30.065
255.000	47.223	-17.492	9.259	46.713	-11.991	29.372
256.000	45.303	-8.204	5.436	45.850	-8.751	27.300
257.000	36.835	17.244	16.958	63.479	1.821	31.329
258.000	39.911	11.711	24.372	53.967	-2.346	28.157
259.000	42.799	1.646	19.791	49.960	-6.515	29.237
260.000	44.952	-5.895	13.564	48.344	-9.287	28.816
261.000	45.355	-3.356	8.372	47.271	-9.771	28.521
262.000	45.464	-7.666	5.459	46.019	-8.221	27.120
263.000	46.397	3.158	2.731	46.553	1.971	22.292
264.000	42.472	1.420	-8.248	44.032	-1.143	22.556
265.000	42.317	-1.431	-0.342	43.805	-2.432	27.943
266.000	37.958	19.915	27.344	53.332	-2.429	27.556
267.000	31.545	20.092	24.367	50.850	1.787	25.231
268.000	34.431	6.256	21.441	46.037	-5.301	25.669
269.000	35.521	6.568	19.156	45.057	-3.966	24.382
270.000	37.465	-2.602	16.482	43.376	-8.510	25.943
271.000	38.222	-3.294	14.321	43.053	-6.856	24.931
272.000	39.528	-6.993	11.809	42.354	-9.818	26.086
273.000	40.226	-6.780	9.960	42.259	-8.833	25.531
274.000	40.407	-7.585	7.612	41.585	-8.763	25.174

E.N	σ_x	σ_y	τ_{xy}	σ_1	σ_2	τ_{max}
275.000	40.702	-7.496	6.695	41.615	-8.409	25.012
276.000	40.323	-5.732	4.556	40.782	-6.190	23.486
277.000	34.772	-7.403	7.114	35.940	-6.570	23.255
278.000	39.737	-1.162	10.825	42.305	-2.894	22.564
279.000	40.005	-0.317	8.389	41.691	-1.993	21.842
280.000	26.115	14.637	21.407	42.568	-3.836	22.192
281.000	30.191	3.320	16.846	38.308	-4.792	21.548
282.000	33.157	-3.082	12.566	37.304	-3.251	22.182
283.000	34.787	-6.008	8.701	36.565	-7.787	22.176
284.000	35.566	-5.566	5.822	35.377	-6.377	21.377
285.000	26.638	16.377	19.806	41.967	1.048	20.463
286.000	32.637	4.782	15.239	37.689	-2.272	19.940
287.000	33.494	-2.086	11.343	36.803	-5.395	21.099
288.000	35.749	-5.132	7.524	38.558	-6.646	21.672
289.000	35.542	-5.647	5.398	36.237	-6.343	21.290
290.000	37.139	-1.489	-2.307	37.284	-3.544	18.473
291.000	39.818	-0.434	-8.256	41.479	-1.227	21.353
292.000	39.982	-1.429	-8.352	41.693	-2.003	21.868
293.000	19.806	10.474	16.377	32.069	-1.889	17.029
294.000	22.664	11.271	15.692	33.527	-2.208	16.663
295.000	24.575	1.317	12.675	30.048	-4.255	17.202
296.000	26.562	1.912	12.134	31.530	-3.158	17.294
297.000	27.582	-3.380	9.430	30.321	-6.019	18.170
298.000	29.127	-2.947	8.939	31.459	-5.270	18.369
299.000	29.541	-4.901	6.515	30.732	-6.092	18.412
300.000	33.465	-4.616	6.483	31.644	-5.777	18.711
301.000	30.466	-4.526	4.333	30.994	-5.055	18.025
302.000	26.763	-5.637	6.885	28.165	-7.039	17.622
303.000	37.250	-0.522	10.355	39.958	-2.197	21.082
304.000	37.716	-1.052	8.374	39.486	-2.963	21.724
305.000	16.409	7.803	13.128	25.921	-1.709	13.816
306.000	23.749	-0.618	10.221	25.027	-3.662	14.337
307.000	23.620	-2.712	7.520	25.616	-4.708	15.162
308.000	25.407	-3.697	5.418	26.391	-4.480	15.434
309.000	16.230	7.026	9.900	22.597	-0.638	10.880
310.000	23.529	-0.422	7.624	23.258	-2.247	12.520
311.000	23.547	-2.953	5.876	24.792	-4.198	14.495
312.000	25.225	-4.111	4.200	25.815	-4.700	15.258
313.000	28.103	-1.171	-2.826	28.373	-1.442	14.928
314.000	37.227	-0.447	-8.278	39.005	-1.331	20.156
315.000	37.649	-1.429	-8.377	39.411	-2.191	20.302
316.000	9.200	3.628	7.286	14.592	-1.264	7.378
317.000	13.827	4.707	8.518	18.928	-0.395	9.562
318.000	15.284	-1.218	5.673	16.979	-3.114	10.597
319.000	17.560	-0.446	6.786	19.921	-2.707	11.314
320.000	19.219	-3.081	4.407	19.094	-3.287	11.825
321.000	20.112	-2.513	5.147	21.228	-3.629	12.428
322.000	22.345	-3.587	3.025	22.717	-3.266	12.360
323.000	18.641	-4.037	5.804	20.229	-5.425	12.827
324.000	34.899	-0.885	9.378	37.354	-1.549	19.426
325.000	35.416	-0.097	8.348	37.281	-1.951	19.521
326.000	8.222	3.066	6.557	12.699	-1.411	7.085
327.000	12.331	-0.574	5.317	14.239	-2.482	8.361
328.000	15.226	-1.090	3.972	15.099	-2.852	9.693
329.000	7.551	-0.832	2.590	8.434	-0.051	4.242

E.N	σ_x	σ_y	τ_{xy}	σ_1	σ_2	τ_{max}
330.000	11.9501	-1.843	2.534	12.400	-2.294	7.347
331.000	14.893	-3.103	1.915	15.094	-3.576	6.179
332.000	19.175	-2.922	-4.275	19.974	-3.722	11.847
333.000	34.757	.455	-8.303	36.673	-3.457	16.785
334.000	35.315	-1.432	-8.398	37.190	-2.806	19.743
335.000	2.595	-1.740	.832	2.797	-1.935	1.861
336.000	6.315	.528	3.278	8.214	-1.670	4.542
337.000	7.386	-2.057	1.229	7.539	-2.711	6.357
338.000	10.295	-1.344	2.733	10.714	-1.964	6.339
339.000	13.624	-2.395	.769	13.460	-2.529	8.736
340.000	11.019	-2.716	3.772	11.987	-3.684	7.835
341.000	22.713	1.139	7.890	24.575	-1.723	17.469
342.000	33.100	-.045	8.320	35.072	-2.017	16.544
343.000	2.251	.216	1.964	2.445	-1.900	2.232
344.000	5.626	-1.137	1.586	5.979	-1.490	3.735
345.000	1.403	-2.296	-1.012	2.106	-3.294	2.730
346.000	5.235	-2.436	-1.022	5.370	-2.570	3.970
347.000	13.244	-4.034	-6.639	12.873	-7.223	12.269
348.000	32.508	.458	-8.334	34.545	-1.580	18.063
349.000	32.933	-1.437	-8.419	34.984	-2.739	17.713
350.000	-1.812	-2.290	-2.596	.556	-4.658	2.607
351.000	1.551	-1.281	-.342	1.594	-1.551	1.551
352.000	1.720	-2.065	-1.869	2.487	-2.833	2.650
353.000	3.292	-1.654	1.643	3.317	-2.577	3.569
354.000	30.772	1.263	5.882	31.902	.153	15.874
355.000	30.762	-.066	6.305	32.055	-2.289	17.527
356.000	-1.962	-.909	-1.189	-.136	-2.736	1.330
357.000	-2.420	-2.425	-3.110	-.682	-3.527	3.110
358.000	1.475	-7.045	-9.954	8.043	-13.612	10.827
359.000	30.523	.455	-5.341	32.652	-1.707	17.194
360.000	30.549	-1.445	-8.441	32.792	-2.588	17.690
361.000	-2.120	-.760	-2.435	1.925	-4.295	2.120
362.000	-6.203	-.168	-1.287	.095	-6.466	3.280
363.000	24.236	1.253	2.315	25.555	-.664	14.330
364.000	28.392	-.186	6.301	30.628	-2.422	16.525

Table 1. All of the values of the stresses from computer